



Universidad
Carlos III de Madrid

FLUORESCENCE LIFE-TIME IMAGING APPROACHES

Bachelor Thesis
Biomedical Engineering

Author: María Ávila González
Tutor: Jorge Ripoll Lorenzo

Leganés, June 2017

Acknowledgements

I would like to express my gratitude to the following people for their support and help during this project.

To my tutor, Jorge Ripoll, for giving the opportunity to work in this project, for his advice, support and for always being accessible when I needed.

To Guillermo Vizcaino, Angelica Corral and Miguel Iñigo, for always being around and available to solve any problem I have encountered. For always welcoming us with a smile and kind words. Working in the lab has been a pleasure.

Thank you to my friends for your endless support, this four years would have not been the same without you.

To Fernando, for living the project with me as if it was your own, for your kind words and your incessant help. Thank you for always believing in me and helping me find the answers even when the questions weren't clear.

Thank you to my family for their support and trust. Thank you for inspiring me each day to keep doing what I love, and for teaching me that everything that is worth it requires a great effort.

ABSTRACT

Imaging techniques using fluorescence as the source of contrast has been widely used in the last decades in biology. Even though fluorescence can give a lot of information, it is sometimes hard to see contrast based on the intensity of fluorescent molecules. This bachelor thesis is based on the idea that contrast in fluorescence images can also be obtained using something different than intensity. In this project, the source of contrast will be the lifetime of a fluorophore, which is understood as the time it takes for an excited electron to go back to its ground state. This property is not affected by concentration, photobleaching or quenching. However, it can vary depending on the microenvironment pH, temperature, viscosity, or binding to other molecules. All of these characteristics make lifetime a very suitable property for studying different dynamic processes in the cells, at the same time as being a good source of contrast in highly autofluorescence samples. The main objective of this thesis was to build a system based on frequency domain lifetime imaging. For its development intensity modulation of a laser as a sine wave at MHz frequencies was required, as well as precise coordination between the laser and the acquisition system (ICCD camera) to see contrast based on lifetime. The project was performed at Universidad Carlos III de Madrid where the implementation of the system took place, as well as its testing to check its capacities and limitations.

Table of Contents

1. INTRODUCTION	15
1.1. Motivation	15
1.2. Fluorescence.....	16
1.2.1. Fluorescence Imaging	19
1.2.2. Fluorescence Lifetime Imaging.....	21
1.2.2.1. Time Domain Lifetime Measurements	22
1.2.2.2. Frequency Domain Lifetime Measurements.....	23
1.2.2.3. Factors affecting lifetime	24
1.3. State of the art.....	26
1.4. Legal Frame.....	27
1.5. Objectives	28
2. MATERIALS AND METHODS	29
2.1. System Components.....	29
2.1.1. Laser	29
2.1.2. Acousto-Optic Modulation.....	30
2.1.2.1. Acousto-Optic Tunable Filter.....	30
2.1.2.2. Multi Digital Synthesizer.....	31
2.1.2.3. Connector DB25.....	33
2.1.3. Emission Filter	34
2.1.4. Lens.....	35
2.1.5. Objective	36
2.1.6. Camera.....	36
2.1.6.1. Signals from the Camera	38
2.1.7. DAQ.....	39
2.1.8. Software Design.....	41
2.2. Final System Assembly	42
2.3. System Initialization Protocol.....	45
3. RESULTS AND DISCUSSION.....	47
3.1. Laser modulation.....	47
3.2. Camera and laser coordination	50
3.3. Testing the system.....	52
4. CONCLUSION.....	56
4.1. Current State of the System.....	56

4.2.	Next Steps	56
5.	SOCIO-ECONOMIC IMPACT	58
6.	PROJECT COST	59
7.	ANNEX	63
7.1.	Lifetime formulas derivation for FD FLIM	63
7.2.	LabView program	64
7.3.	Matlab Code	67
7.4.	Reference Sheet	68
7.5.	Timeline of the project	70
8.	BIBLIOGRAPHY	71

List of figures

Figure 1: Perrin-Jablonksi diagram from [4]	16
Figure 2: Total spin number and multiplicity in singlet and triplet state from [4]....	17
Figure 3: Example of fluorophore absorption and emission profile from [5].....	18
Figure 4: Basic set up for a fluorescence microscope from [7]	19
Figure 5: Fluorescent image of cell showing actin filament (green), nucleus (blue) and mitochondria (yellow) from [9].....	20
Figure 6: Basic representation fluorescence intensity image vs. FLIM from [6]	21
Figure 7: TD lifetime measurements from [6].....	22
Figure 8: TCSPC measurements from [12].....	23
Figure 9: FD lifetime measurements from [6]	23
Figure 10: (A) MRL-III-671/1~200mW laser from [23]; (B) CPS532 - Collimated Laser Diode Module, 532 nm, 4.5 mW, Round Beam, Ø11 mm Housing from [24]	29
Figure 11: (A) Schematic of Acousto-Optic Modulation from [25] (B) Separation on the laser beam in different diffraction orders from [26]	30
Figure 12: AOTFnC-400.650-TN from [28].....	31
Figure 13: Multi Digital Synthesizer (MDS) from AA Opto-electronic from [28].....	31
Figure 14: (A) AOTF set up; (B) and (D) Different diffraction orders for the green and red lasers, with all channels ON; (C) and (E) 0 th and 1 st diffraction order (transmitted and diffracted light).....	32
Figure 15: (A) Diffracted light modulation from [25] (B) Working mode of the MOD IN and BLANKING signals from [28].....	33
Figure 16: (A) connector DB25, (B) Connections made in different pins.....	33
Figure 17: 700nm 50mm Diameter, OD 2 Longpass Filter from [29]	34
Figure 18: Spectrum of the excitation source, absorption and emission of the fluorophore from [30], and emission filter.	35
Figure 19: AC254-100-A-ML - f=100 mm, Ø1" Achromatic Doublet, SM1-Threaded Mount, ARC: 400-700 nm from [31]	35

Figure 20: 25,0 mm C-Mount Objektiv Pentax C2514-M (KP) / Ricoh FL-CC2514-2M - 1.4 / 25mm from [32]	36
Figure 21: Intensified CCD camera from [33]	37
Figure 22: Signals from the camera from [34]	38
Figure 23: CH1 (yellow): Output A, CH2 (blue): Gate monitor	39
Figure 24: USB-6341, National Instruments from [36].....	40
Figure 25: Schematic for the wiring process.....	40
Figure 26: (A) Final System Assembly: A-Detection system, B-MDS, C-DAQ. (B) Close up to the detection system: D-Laser, E-AOTF, F-Lens, G&H- Mirrors to redirect the path of the diffracted light, I- ICCD camera, J- Emission filter, K- Objective.	43
Figure 27: Schematic drawing of final system assembly.....	44
Figure 28: Images obtained from a video showing the laser modulation. Frequency of modulation: 10Hz.....	47
Figure 29: (A) f=1kHz, (B) f=10kHz, (C) f=100kHz, (D) f=400kHz. CH4 (blue): signal measured from analog output from the DAQ. CH3 (purple): signal measured from RF OUT from MDS.	48
Figure 30: (A) Laser, (B) AOTF, (C) Photodetector.....	49
Figure 31: In all images, the blue signal (CH4) corresponds to the signal generated by the DAQ, and the purple signal (CH3) corresponds to the signal obtained from the photodetector. Different frequencies were measured (A) f=500Hz, (B) f=1kHz, (C) f=100kHz, (D) f=300kHz.....	49
Figure 32: Same exposition time (20ms) and gate delay (10ms) were used in all images. The delay between Output A (CH1) and the sinusoidal wave (CH4) varies in each image (ΔX).	50
Figure 33: Sequence of images obtained from a video of the acquisition process at (A) 10kHz and (B) 300kHz. The red arrow points to the gate monitor	51
Figure 34: Normalized images of different modulation frequencies (A) f=1000Hz, (B) f=10kHz, (C) f=100kHz, (D) f=200kHz, (E) f=300kHz.....	53
Figure 35: Simulations performed showing modulation and phase angle shift at different modulation frequencies	54
Figure 36: Control window of LabView Program.....	64
Figure 37: Terminal window of LabView program	64
Figure 38: Terminal window LabView program (1).....	65

Figure 39: Terminal window LabView program (2).....	66
Figure 40: Terminal window of LabView program (3).....	66
Figure 41: Timeline of the project.....	70

List of tables

Table 1: System components associated costs (1).....	59
Table 2: System components associated costs (1).....	60
Table 3: Technical Equipment associated costs.....	61
Table 4: Human Resources associated costs.....	61
Table 5: Total cost of the project	62

Acronyms

FLIM: Fluorescence Lifetime Imaging Microscopy

TD: Time Domain

FD: Frequency Domain

TCSPC: Time correlated Single Photon Counting

FRET: Förster Resonance Energy Transfer

ICG: Indocyanine Green

AOTF: Acousto-Optic Tunable Filter

RF: radio frequency

DAQ: Data Acquisition

DDG: Digital Delay Generator.

1. Introduction

1.1. Motivation

Different modalities are widely available for in vivo medical imaging, such as X-ray, computed tomography (CT), magnetic resonance imaging (MRI) and ultrasound (US). In each of these modalities different contrast agents are used, as iodine compounds (X-ray), paramagnetic metals (MRI) or microbubbles (US), however, for the most part, they are non-targeted compounds, i.e. they don't specifically bind to the target molecule, producing detectable signal constantly. Although these techniques have been used to diagnose and monitor many different diseases, a new approach where background signal is reduced and target signal increased is desired, which will lead to an increased in target-to-background ratio, enhancing sensitivity and specificity.

This new approach where target signal is maximized has been implemented thanks to the development of fluorescent activatable probes in optical imaging. Fluorescent activatable probes are defined as compounds that only emit light under specific situations, such as enzymatic reactions, changes in the pH or oxygen concentration in the microenvironment, or binding to a specific molecular target. Therefore, they are "off" while none of these conditions take place, greatly reducing the background signal. Cancer cells have distinctive microenvironment and cell surface compared to those of normal cells, which makes fluorescent activatable probe suitable for targeted imaging. In addition to this, fluorophores can be conjugated with molecules that give them specificity, which ensures signal in the desired target [\[1\]](#).

However, if intensity fluorescence measurements are being taken, it is important to have in mind that UV light excitation can lead to cell damage, while visible light excitation is only suitable for surface imaging (for green and blue excitation) due to its low penetration ability, and around 600nm excitation causes excessive autofluorescence. Near Infrared (NIR) excitation (650-900nm) gives deepest tissue penetration as well as lower autofluorescence being the suitable excitation for in vivo applications [\[2\]](#).

Fluorescence activatable probes are a newly developed tool to increase signal-to-background ratio, but it is not the only way to increase contrast. If instead of

imaging the intensity of the emitted fluorescence, the rate at which fluorescence took place is imaged, a new source of contrast would be found. In this bachelor thesis Fluorescence Lifetime Imaging (FLI) was used, where lifetime measurement is used as the source of contrast. Since lifetime is independent of concentration, excitation light and light scattering, if tissue autofluorescence has a different lifetime than the fluorescent probe being image, FLI measurements will allow for easy removal of background noise without the need of special fluorophores [3].

1.2. Fluorescence

Different processes take place when light interacts with matter. Light can be scattered, absorbed or emitted. For the purpose of this bachelor thesis only light absorption and emission will be studied, since light scattering will not be necessary in order to understand the basics concepts of the experiment performed.

Light absorption occurs when light is able to excite some electrons to move from the ground state to an unoccupied orbital in the excited state. Since this high-energy state is very unstable, there are several ways for the electron to go back to its ground state, and photons can be emitted in the process (radiative de-excitation). An easy and visual way to see the different possibilities the electron has to go back to its ground state, are represented in a Perrin-Jablonski diagram.

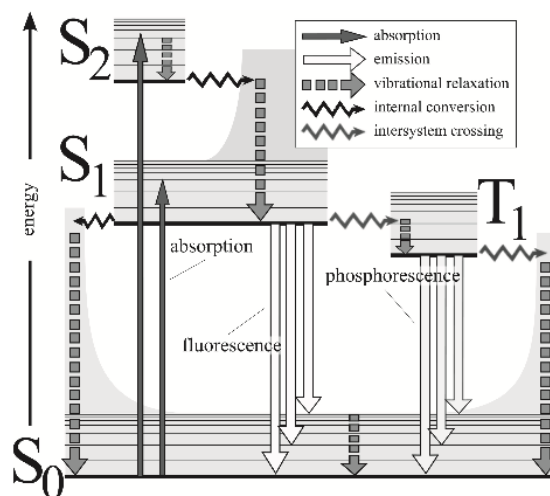


Figure 1: Perrin-Jablonski diagram from [4]

Depending on the rate at which the emission occurs we can distinguish between *fluorescence and phosphorescence*. Fluorescence has lifetimes in the nanosecond to hundred nanoseconds scale, while phosphorescence processes have longer lifetime around the 10^{-6} to one-second range. To understand the time difference between these two phenomena a look into the spin number and multiplicity of the excited states is required.

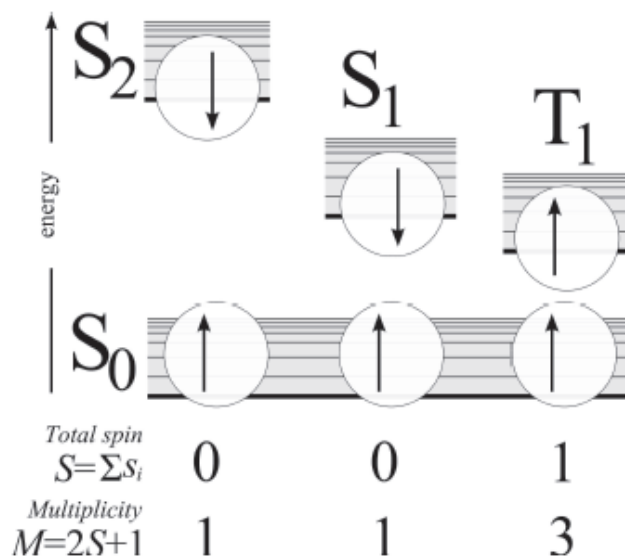


Figure 2: Total spin number and multiplicity in singlet and triplet state from [4].

As it can be seen in the figure above two different states can be differentiated. The first one corresponds to a singlet state ($S=0$, $M=1$). The second one is a triplet state ($S=1$, $M=3$), and it is produced when an electron in the singlet state undergoes a spin reversal, which increases the total spin number and the multiplicity, which makes it have a lower energy according to Hund's rule. Transitions from T_1 to S_0 through non-radiative processes (where no photons are emitted) are very efficient and therefore radiative emission (phosphorescence) rarely occurs.

Fluorescence is the light emission resulting from a transition between a singlet-excited state (S_1) to a ground state (S_0), while phosphorescence takes place during the transition from a triplet state (T_1) back to the ground state.

Another important feature to take into account regarding fluorescence (and also phosphorescence) is that the emission wavelength maximum is always going to be higher than the absorption one since some energy has been lost through vibrational relaxation (*Stokes Shift*) [4].

(Recall the energy of a photon can be calculated as $E = \frac{hc}{\lambda}$)

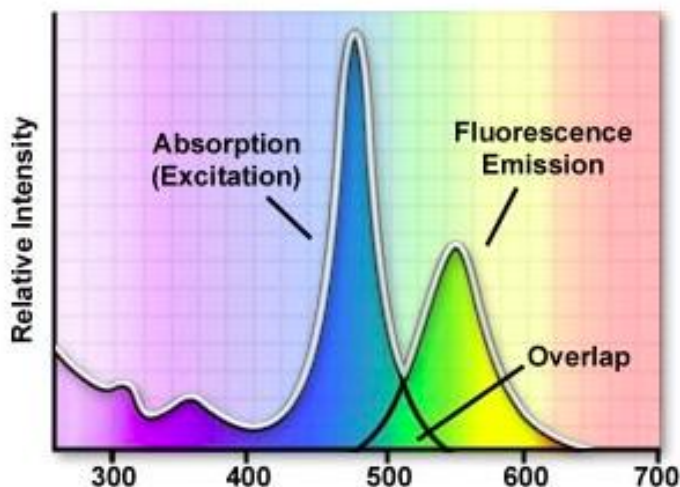


Figure 3: Example of fluorophore absorption and emission profile from [5]

The two properties that best characterize a fluorophore (molecule that emits light through fluorescence) are lifetime (τ) and quantum yield (Q). Lifetime can be understood as the “average time the molecule spends in the excited state prior to return to the ground state” [6], and quantum yield refers to the “number of emitted photons relative to the number of absorbed ones” [6]. These two properties have mathematical expressions that take into account the radiative de-excitation rate (Γ), as well as the non-radiative de-excitation (k_{nr}).

$$\tau = \frac{1}{\Gamma + k_{nr}} \quad Q = \frac{\Gamma}{\Gamma + k_{nr}}$$

1.2.1. Fluorescence Imaging

The use of fluorescence as a way of obtaining new and more informative images was a breakthrough in the microscopy field, leading to the development of several techniques that use fluorescence. Some of these techniques are epifluorescence microscopy, confocal microscopy, multiphoton fluorescence excitation microscopy and fluorescence lifetime imaging to name a few.

Fluorescence microscopy is especially important in biology for different reasons. It allows for high contrast images, provided by the fluorescence emission against a black background. High specificity is achieved, since biological samples can be genetically or chemically modified to express fluorescent labels where desired. Moreover, it allows for live cell imaging, making it a very useful technique to understand cell processes in vivo and in real time. It can also be used to examine physiological concentration of different ions, to detect the presence of specific molecules or cells, or act as a marker for specific cellular structures

The main components of a basic fluorescence microscope are represented in *Figure 4*.

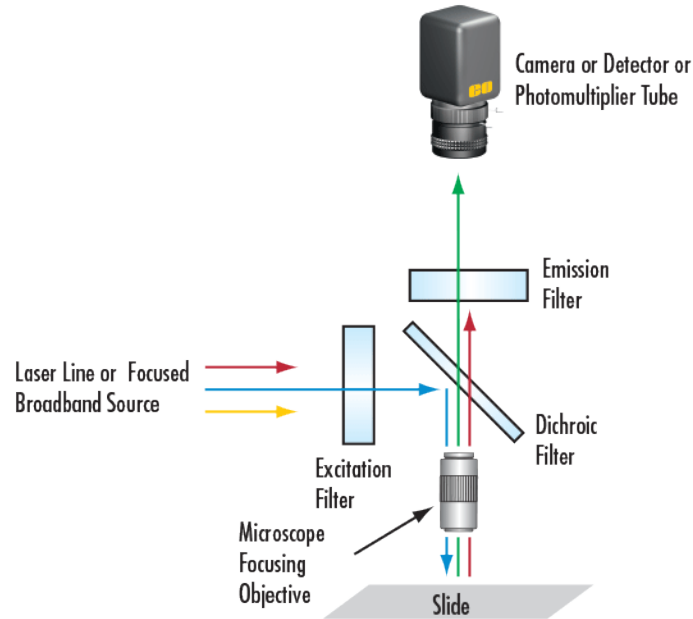


Figure 4: Basic set up for a fluorescence microscope from [7]

It is important to notice the need of different filters in order to obtain a fluorescence image. The excitation filter allows only for the transmission of the excitation wavelength, which is different for each fluorophore. On the other hand, the emission filter will only let the wavelength corresponding to emission, which is also a characteristic feature of each fluorophore, to go through it and get to the detector. This imaging technique can be done thanks to the difference in wavelength for the absorption and emission, described previously as Stokes Shift, allowing removal of the excitation wavelength on the final image.

Since filters have to match the specific absorption and emission curves of each fluorophore, if two different fluorophores are present in a sample, in a simple set up filters will only allow for the imaging of one of them. By changing the set of filters to match each specific fluorophore, images like the one shown in *Figure 5* can be obtained by merging the individual images of the different fluorophores afterwards [8].

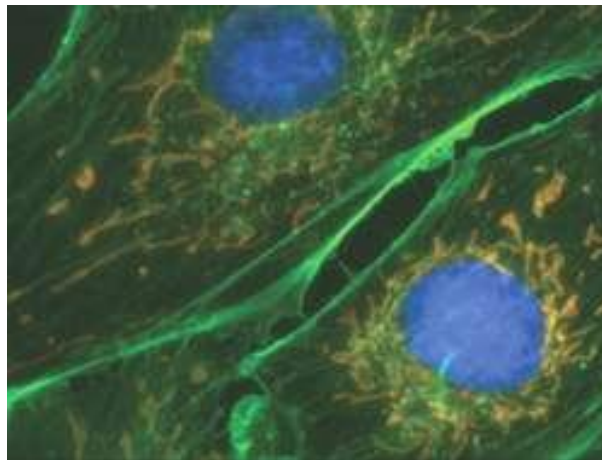


Figure 5: Fluorescent image of cell showing actin filament (green), nucleus (blue) and mitochondria (yellow) from [9]

Even though this intensity based methods have been critical for biological studies and have given information about cellular morphology, measurement of molecule concentration inside the cell and protein binding processes to give some examples, fluorophores are highly subjected to the local environment, and can photobleach, quench or modify its intensity as a decrease in fluorophore concentration. Photobleaching is the irreversible damage of the fluorescent molecules due to overexposure of the sample, quenching is produced when there is a transfer of

energy to another molecule (acceptor), which resides physically close to the excited fluorophore (donor)[\[10\]](#).

1.2.2. Fluorescence Lifetime Imaging

Fluorescence Lifetime Imaging Microscopy (FLIM) is a type of fluorescence microscopy but the contrast in this technique is given by measuring the lifetime of the sample in each region. This makes it a time-resolved method that can provide more information than steady-state ones (intensity based).

If there were two different regions on a sample, with the same fluorescent molecule present, but with a different concentration of some molecules, when comparing these two methods on a single image (*Figure 6*) two very different images would be obtained. Measuring the intensity of the fluorescence emission it might not be possible to differentiate between the two regions, since the quantum yield might be the same, but if what was been image was the lifetime instead, a clear picture that a different environment was affecting both regions is obtained, since lifetime is highly dependent on the local environment factors such as temperature, pH, oxygen concentration... Factors affecting the lifetime of fluorophores will be discussed in more detailed in the following sections of this work.

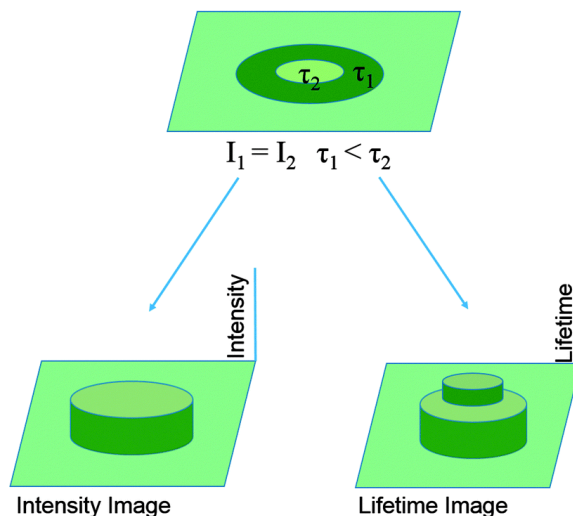


Figure 6: Basic representation fluorescence intensity image vs. FLIM from [\[6\]](#)

Lifetime is an intrinsic property of the fluorophore, i.e. it is not affected by the amount of fluorophore present. This insensitivity to intensity-based artifacts such as

photobleaching, detection gain setting or modifications in the excitation sample intensity makes it more suitable than steady state fluorescence for many applications[11]. However, FLIM measurements are harder to get.

There are two main ways of measuring lifetime, time domain (TD) or frequency domain (FD) methods, which will be further explained in the following section.

1.2.2.1. Time Domain Lifetime Measurements

Using Time Domain methods in order to calculate the lifetime of a fluorophore a pulse excitation shorter than the lifetime of the fluorophore under study is required. The lifetime will be calculated using the slope of the logarithmic intensity vs. time plot (*Figure 7*).

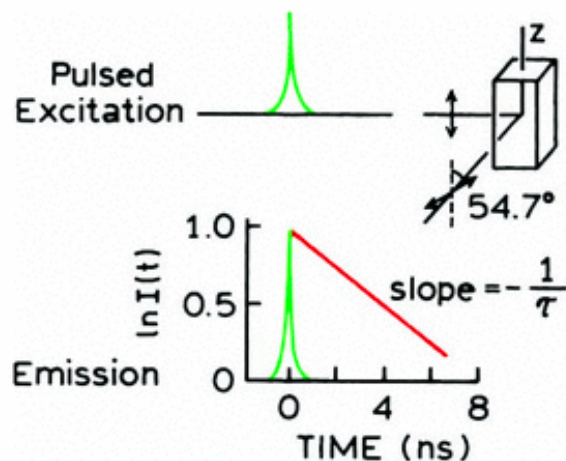


Figure 7: TD lifetime measurements from [6]

The most common approach for time-domain FLIM is Time correlated Single photon counting (TCSPC), where after the pulse excitation the time until the first photon reaches the detector is measured. After several pulse excitations and corresponding photon measurements a histogram representing the photon distribution in terms of delay can be obtained. The histogram represents the fluorescence decay, which follows an exponential law.

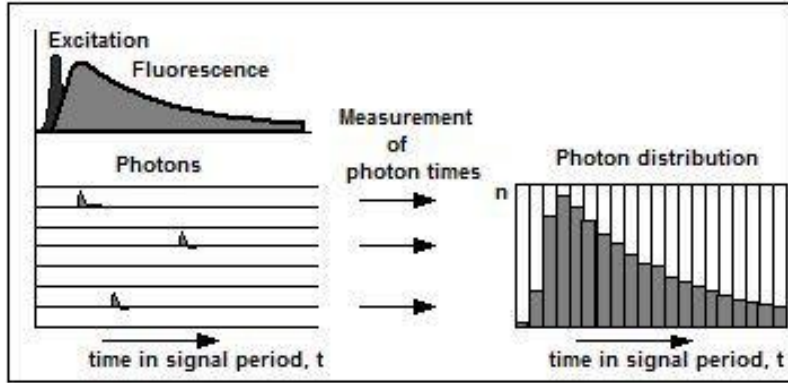


Figure 8: TCSPC measurements from [12]

No further details will be given about this technique since it is out of scope of this work.

1.2.2.2. Frequency Domain Lifetime Measurements

Frequency Domain methods rely on a modulated excitation rather than the pulse excitation used in TD. The sample is excited with sine wave amplitude-modulated light and the modulation frequency has to be of the order of megahertz for the frequency to be comparable to the lifetime of nanoseconds of fluorescence emission. Fluorescence emission will have the same frequency as the excitation one, but a phase-shift and modulation will be seen (Figure 9). The phase shift and demodulation can be used to calculate τ .

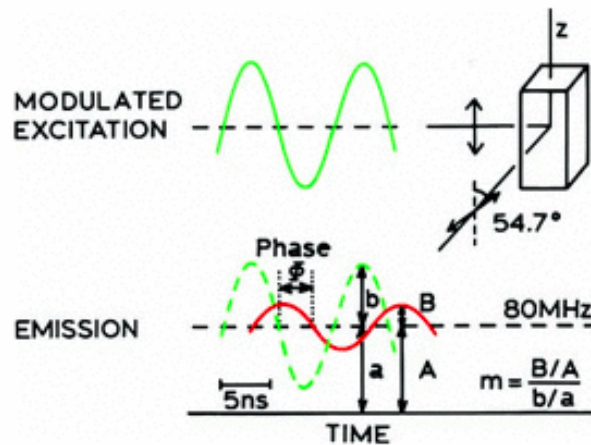


Figure 9: FD lifetime measurements from [6]

The formulas require for estimating the lifetime using the phase shift and the demodulation measurements are the ones below, where ω is determined by the modulation frequency, ϕ corresponds to the phase shift between the excitation and the emission and m is understood as the demodulation of the emission with respect to the excitation.

$$\tan(\phi) = \omega \tau_{\phi} \rightarrow \tau_{\phi} = \omega^{-1} \tan(\phi)$$

$$m = \frac{1}{\sqrt{1 + \omega^2 \tau_m^2}} \rightarrow \tau_m = \frac{1}{\omega} \sqrt{\frac{1}{m^2} - 1}$$

(Derivation of these formulas can be found in the *Annex: 7.1 Decay time formulas derivation for FD*)

The modulation frequency can be modified depending on the lifetime of the fluorophore, but it is important to take into account that the modulation frequency has to be comparable to the lifetime, which means that

$$\frac{1}{\text{Modulation Frequency}} \propto \text{lifetime}$$

1.2.2.3. Factors affecting lifetime

As it was mentioned in the previous sections, lifetime is an intrinsic property of the fluorescent molecule, and it is not dependent on factors that modify the intensity, such as fluorophore concentration, photobleaching, neither on the duration of the excitation. But there are many other factors that can modify the lifetime of a fluorophore. Lifetime is estimated based on the radiative de-excitation rate as well as the non-radiative de-excitation rate, therefore modifications of these two properties will result in a variation of the lifetime. These two rates are affected by fluorophore conformational changes.

Many fluorophores contain double bonds that after excitation become single bonds. This change between double and single bonds affects the molecule flexibility, since double bonds are more rigid. This effect can also be seen as a result of temperature, viscosity or polarity changes of the environment. If the temperature is decreased or

the viscosity of the medium is increased, lifetime has been proved to increased. The increase is attributed to the inability of the excited electron to go back to the ground state through non-radiative processes.

Intersystem crossing can be another reason for lifetime variations. When fluorescence was explained at the beginning the thesis, it was noted that transitions between S1 and T1 states were possible by spin reversal (leading to phosphorescence).

Another important factor is Förster Resonance Energy Transfer (FRET). FRET is defined as the energy transfer between two light sensitive molecules[13]. For the energy transfer to take place the molecules need to be at an appropriate distance, and their wavelength spectra need to overlap. This is due to the fact that the emission of one of the molecules will be taken as the excitation of the other one, therefore the emission of the donor need to be able to excite the acceptor. If lifetimes of this process are looked at, it will be seen that the donor molecule lifetime will dramatically decreased, while the lifetime of the acceptor will remain the same. This process can be used as a way of measuring distances between different molecules. At distance smaller than the ones available for FRET, Dexter Electron Transfer can be used[14].

Lifetime variations due to environmental changes makes FLIM a very useful tool for the study of intracellular processes among many other applications in chemistry and material science.

1.3. State of the art

The development of time-resolved techniques has been highly limited in the 20th century by slow electronics. Once faster electronics were available, different approaches to measure lifetime were developed. Many different groups have come up with different ideas to implement time and frequency domain FLIM. Some examples of the latest achievements in the field will be given, as a way of giving some background on how far these techniques have gone.

Zhong et. al (2003) were able to demonstrate the ability of measuring lifetime variations in an oxygen-sensitive dye in solution and in living cells, which could be very useful as a way of quantifying intracellular oxygen concentration. FLIM system was implemented by using low repetition rate laser and a wide-field ICCD camera for the detection process [15]. Some of the main applications of fluorescence lifetime imaging is the ability to measure dynamic processes. By combining different techniques such as FLIM and FRET, study of protein interaction in cells was reported. Elangovan et. al (2002) developed a FRET-FLIM microscopy that allows for detection of time-resolved images of donor in the absence or presence of acceptor. They specifically use it to quantify the dimerization of the transcription factor CAATT/enhancer binding protein alpha in living pituitary cells. Since only the donor fluorophore lifetime is measured with and without the acceptor, they were able to calculate the distance between interacting proteins inside cells with great precision thanks to the nanometre resolution provided by FRET, and the nanosecond resolution given by FLIM [16]. Many other studies have exploited the combined advantages of using FRET-FLIM techniques. Calleja et. al (2003) were able to monitor conformational changes of proteins in cells using a GFP-YFP fusion protein that allows for FRET measurements. If any conformational changes took place, the lifetime would change [17].

Although many researchers have used time domain FLIM, there are many other projects where frequency domain FLIM was chosen. Wagnieres et. al (1997) made use of the lifetime fluorescence changes in healthy and diseased tissue, specifically in cancerous tissue. The image was obtained using an endoscope and photocathode intensifiers, and lifetime fluorescence in each pixel was calculated almost at real time [18]. Another example of frequency-domain fluorescence lifetime confocal microscopy was implemented by Booth et. al (2004) by using a switched diode laser as the illumination system [19].

1.4. Legal Frame

During the project, different lasers were used always following the laser safety procedures. Laser beam was always controlled and limited by physical barriers, since other people were working in the laboratory at the same time. Glasses were worn when working with the laser. Regarding the alignment of the laser beam it was done at a height different than the standing or sitting position, to avoid unwanted eye contact with the laser beam by chance [\[20\]](#),[\[21\]](#).

Fluorophore regulation for animal and human ones is quite different. A review regarding the most used fluorophores (such as Alexa Fluor 488 and 514, BODIPY FL, BODIPY R6G, Cy 5.5, Cy 7 and ICG to name a few) was made in order to determine their toxicity and possible application in human studies. Many different fluorophores are used in animal studies but the two FDA has only approved two fluorophores for human use, Indocyanine Green (ICG) and fluorescein. Even though ICG has been reported to produce toxicity, the doses given to humans are well below the toxic amount, since low doses are enough for the therapeutic means [\[22\]](#).

1.5. Objectives

This bachelor thesis was focused in the construction of a system that will be able to acquire lifetime measurements using a frequency domain fluorescence imaging approach. The idea behind this works lies in the new information provided by studying the lifetime of a fluorophore, instead of its intensity, since lifetime is not affected by extrinsic properties such as fluorophore concentration, duration of the excitation or photobleaching. The system will be used in future works to look for contrast in fluorescence images using an estimation of the lifetime, instead of relying on the usual intensity based fluorescence systems, where contrast sometimes can be difficult to obtained.

The main goal of this project was to construct the system from scratch and test it, to know its capacities and limitations. The development of this system presents several difficulties: (1) being able to intensity-modulate the laser as a sine at high frequencies, in the MHz range; (2) coordination between the laser and the acquisition system (ICCD camera) and (3) acquisition of images in a precise enough way that allows for measuring contrast based on lifetime.

This general objective can be divided into the following specific objectives:

1. Understand how each of the components works.
2. Assembly of all the different components of the system.
3. Make the proper connections to coordinate all of the devices.
4. Establish an initialization protocol to facilitate future use of the system.
5. System testing.

2. Materials and Methods

2.1. System Components

In order to be able to understand the how the whole system was implemented, an explanation of the single components and how they work together is required. In order to be able to acquire lifetime images, precise coordination of the different components is needed.

2.1.1. Laser

The illumination system chosen for this work was laser light. Lasers are coherent light sources, in the spatial and temporal term, which makes them suitable for precise point excitation over great distances, as well as being monochromatic, since only one wavelength can be generated. Thanks to this property no excitation filter is require in this work, since the illumination system will adequately provide only one excitation wavelength. The two lasers used during this project had wavelengths of 671nm (red) and 532nm (green) but the final images obtained with the fluorophore were performed using the 671nm laser.

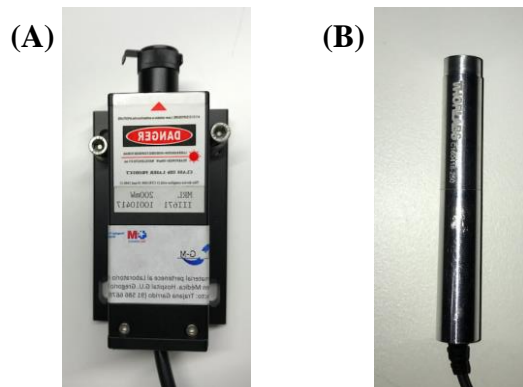


Figure 10: (A) MRL-III-671/1~200mW laser from [23]; (B) CPS532 - Collimated Laser Diode Module, 532 nm, 4.5 mW, Round Beam, Ø11 mm Housing from [24]

2.1.1.2. Acousto-Optic Modulation

Acousto-Optic Modulation is a technique used in many different settings mainly to control lasers. They are based on the interaction effect between light and sound in a transparent material. One of the most common materials used is TeO_2 crystals. A radio frequency (RF) signal is applied to a piezo-electric transducer, which creates sound waves in the TeO_2 crystals. The sound wave travelling through the material creates bands inside the material with different refractive index (Figure 11 (A)) [25]. This difference in refractive index in the different bands allows for the separation of the laser beam in different diffraction orders (Figure 11(B)) [26]. Therefore, it is possible to separate the incident light into diffracted and transmitted light. Since all part in the device are fixed, it allows for laser modulation in a very reliable, stable and fast way [27] which is very important when fluorescence lifetime images are going to be taken.

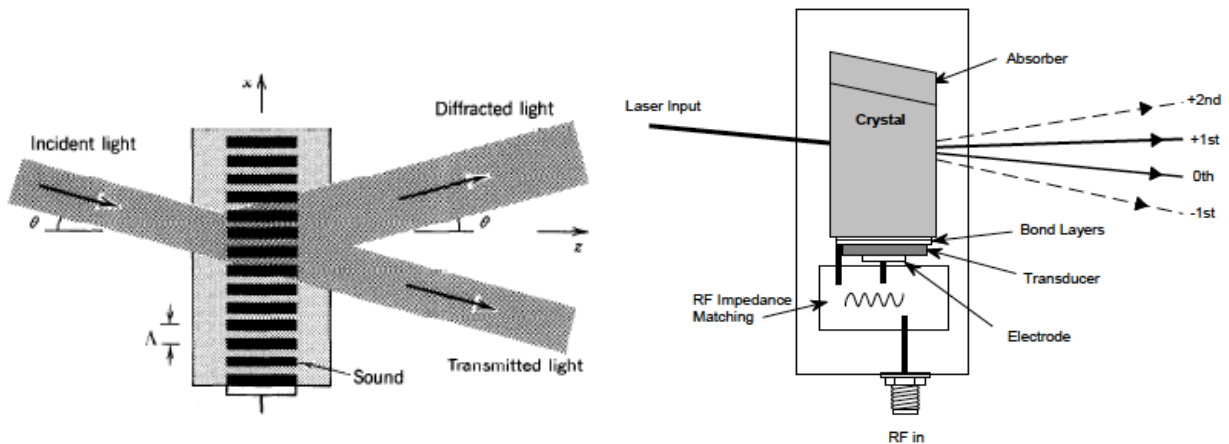


Figure 11: (A) Schematic of Acousto-Optic Modulation from [25] (B) Separation on the laser beam in different diffraction orders from [26]

2.1.1.2.1. Acousto-Optic Tunable Filter

As a way of controlling the laser amplitude modulation, an Acousto-Optic Tunable Filter (AOTF) was used. It was obtained from AA Opto-electronic. It is made of an anisotropic medium of TeO_2 -S, which works in the optical wavelength range between 400-650 nm and has an active aperture of $3 \times 3 \text{ mm}^2$. It allows for high separation angle between orders 0 and 1 of around $\geq 4^\circ$, and it comes with temperature stabilization. Thanks to the AOTF it is possible to control the amplitude

of the diffracted wavelength. In this specific set up, the diffracted wavelength needs to be modulated as a sine wave. SMA Connector for RF Input and SMC Connector for Thermal regulation supply were connected to the Multi Digital Synthesizer (MDS).



Figure 12: AOTFnC-400.650-TN from [28]

2.1.2.2. Multi Digital Synthesizer

In order to control the AOTF an RF signal had to be applied to the piezo-electric transducer. The RF driver used was a Multi Digital Synthesizer (MDS) from AA Opto-electronic. It is composed of eight different channels that can provide RF frequencies between 74-158 MHz's.

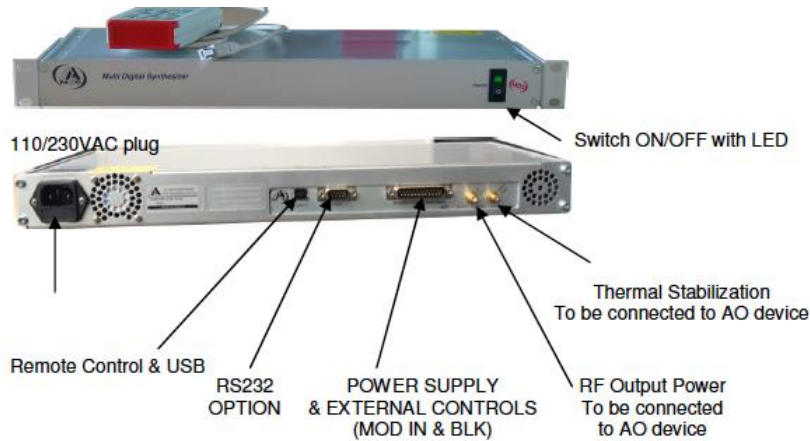


Figure 13: Multi Digital Synthesizer (MDS) from AA Opto-electronic from [28].

There are two ways of using the MDS, through external or internal control. In the Internal mode, the user is able to control the different channels through a USB, Remote control or RS232 communication. In this project External mode was used,

since better performance is expected according to the manufacturer. For external control the use of a connector DB25 was required.

Before changing to external mode, it was required to select the adequate channel, that gave the best separation between the zero and first order diffraction, using the internal mode (Figure 14). Laser light has to enter the AOTF with an angle to allow for separation between the transmitted and diffracted light, and this angle will be different depending on the laser wavelength (Bragg condition).

When all the channels were on, many diffraction orders were seen, however, as it can be seen, not all points are equally brighter (Figure 14 (B) & (D)). The channel chosen was the one giving brightest spot (Figure 14 (C) & (E)). Two different lasers were used, for the 671nm laser the first channel was used with a frequency of 74,5 MHz, while for the 532nm laser the first channel was also used, but with a frequency of 124MHz. Thanks to the software developed by AA Opto-electric the frequency in the different channels can be chosen by the user, which is very helpful, since when external mode is used, each pin on the DB25 connector corresponds to a specific channel of the MDS, therefore only one channel needs to be prepared for external control.

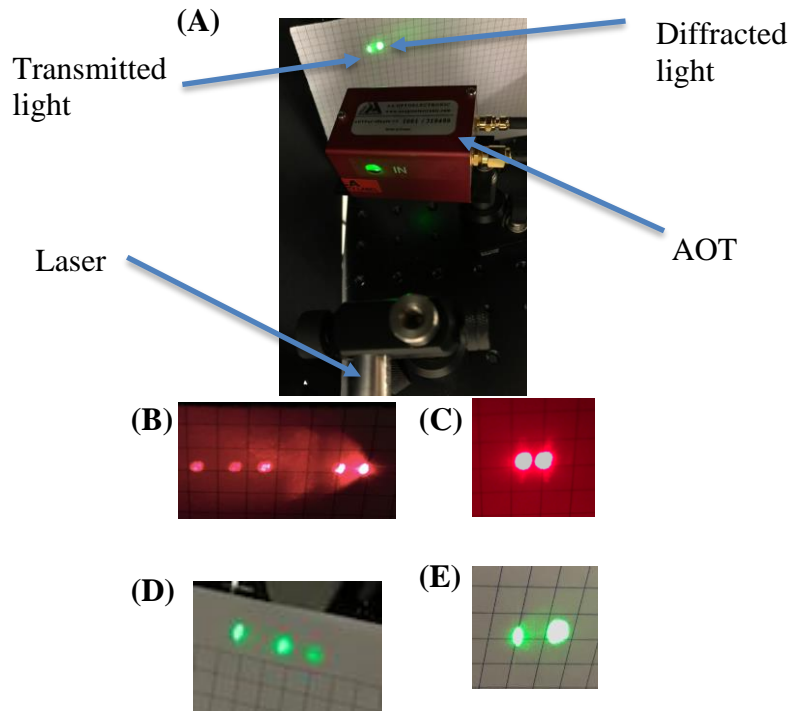


Figure 14: (A) AOTF set up; (B) and (D) Different diffraction orders for the green and red lasers, with all channels ON; (C) and (E) 0th and 1st diffraction order (transmitted and diffracted light)

2.1.2.3. Connector DB25

Connector DB25 was used in order to be able to perform external control of the MDS device. Two different inputs have to be given for external mode. The first one is the Modulation inputs (MOD IN) that allows choosing any type of signal for the RF applied to the piezo-electric. If instead of a constant RF signal, the RF signal oscillated following a sinusoidal wave, it would allow for laser amplitude modulation as a sine wave, since the crystal media will have changes in the index of refraction in a sinusoidal way (Figure 15(A)). In this project that was the goal, since intensity modulation of the laser is needed for FD FLIM. The second input that had to be controlled was Blanking input, which need to be at a high level to allow modulation inputs to operate. Figure 15(B) shows the RF output frequency depending on Modulation Input and Blanking.

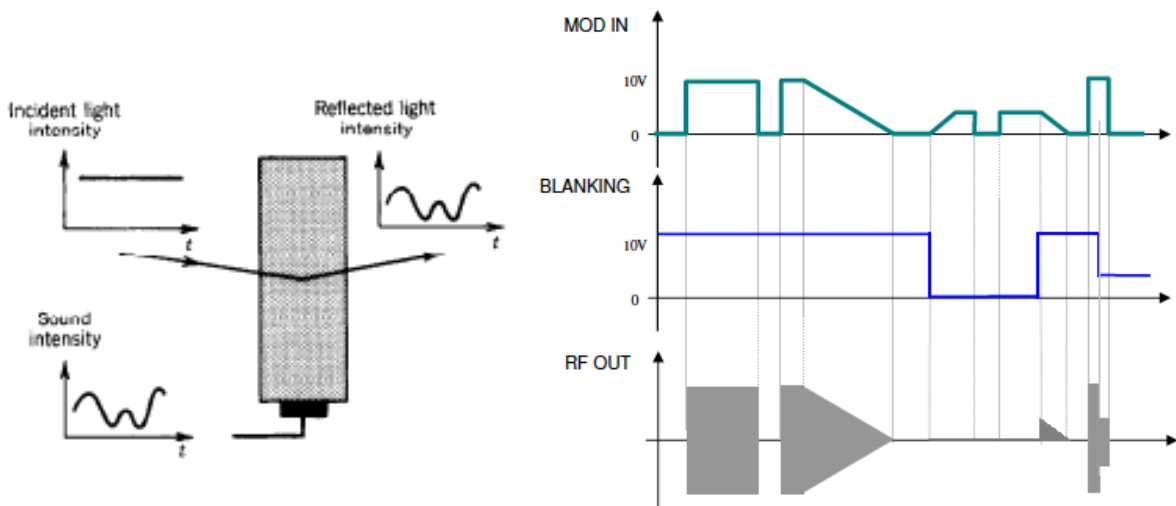


Figure 15: (A) Diffracted light modulation from [25] (B) Working mode of the MOD IN and BLANKING signals from [28]

In order to perform these operation different pins of the DB25 were used:

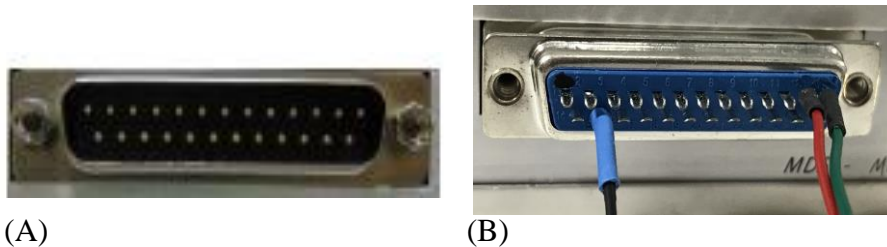


Figure 16: (A) connector DB25, (B) Connections made in different pins

- *Pin 13 (Green cable) for BLANKING input (5V).*
- *Pin 12 (Red cable) for MOD IN which correspond to Channel 1 in the MDS. (In this project, a sinusoidal wave generated using a DAQ was input through this pin).*
- *Pin 15 (Black cable) for Ground.*

Further details on how this was connected to the other parts of the system will be given.

2.1.3. Emission Filter

An emission filter is required in order to precisely retrieve only fluorescence emission. The emission filter will remove any undesired light (as the excitation light from the laser) getting to the camera while letting fluorescence light go through. The emission filter is place right before the objective in the camera (Figure 27), and depending on the emission spectra of the fluorescent probe a different filter will be required. In this case a fluorophore (CF680-Maleimide) with absorption maxima at 681nm and emission maxima at 698 nm was used. The filter chosen was a long pass filter that transmit only wavelengths longer than 700nm.

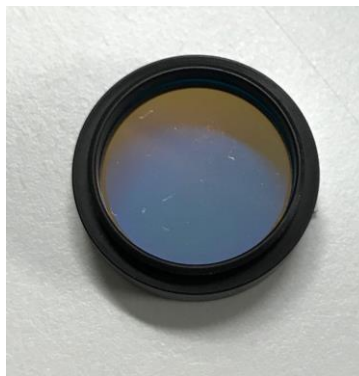


Figure 17: 700nm 50mm Diameter, OD 2 Longpass Filter from [\[29\]](#)

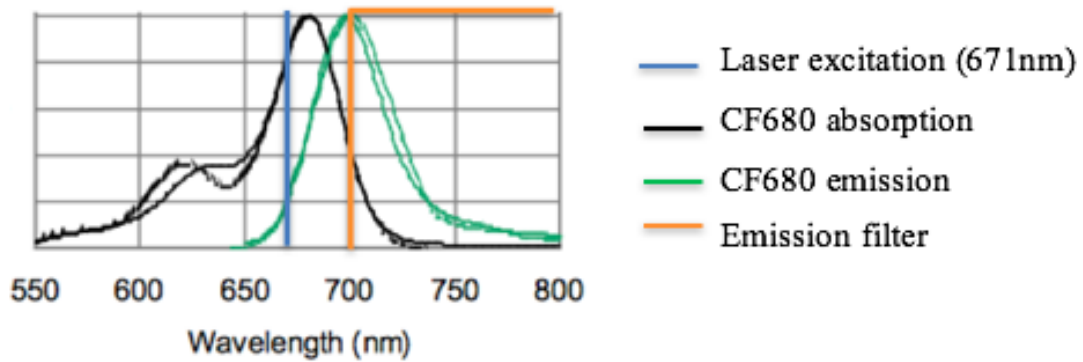


Figure 18: Spectrum of the excitation source, absorption and emission of the fluorophore from [30], and emission filter.

2.1.4. Lens

A 100 mm of focal length lens was used in order to increase the laser beam size, to achieve a more homogenous illumination over the sample. Since homogenous illumination of a medium size region was desired, a convergent lens was used, to prevent the illumination point to be too wide.



Figure 19: AC254-100-A-ML - $f=100$ mm, $\text{Ø}1''$ Achromatic Doublet, SM1-Threaded Mount, ARC: 400-700 nm from [31]

2.1.5. Objective

The objective was used to capture the incident light and focused it to get an image. It is composed of different lenses, that allows to capture the image at maximum focus and constant collimation. The one used in this project was purchase from PENTAX.



Figure 20: 25,0 mm C-Mount Objektiv Pentax C2514-M (KP) / Ricoh FL-CC2514-2M - 1.4 / 25mm from [\[32\]](#)

2.1.6. Camera

The camera used as the detection system was the ICC DH334 T-18U-03 (from ANDOR iStar). The 334 corresponds to the CCD matrix of 1024 x 1024 pixels of 13 μ m pixel size, 18 is the size of the intensifier diameter, U means that it is prepared for Ultra-Fast Gating, and 03 determines de image intensifier material, which in this case corresponds to a W-AGT photocathode and P43 phosphor. To understand better why this camera is suitable for the detection of fluorescence lifetime images, a brief explanation on what a ICC camera is will be given.

Intensified CCD cameras differ from CCD ones in that they have an image intensifier with a photocathode, microchannel plate (MCP) and a phosphor screen (Figure 21).

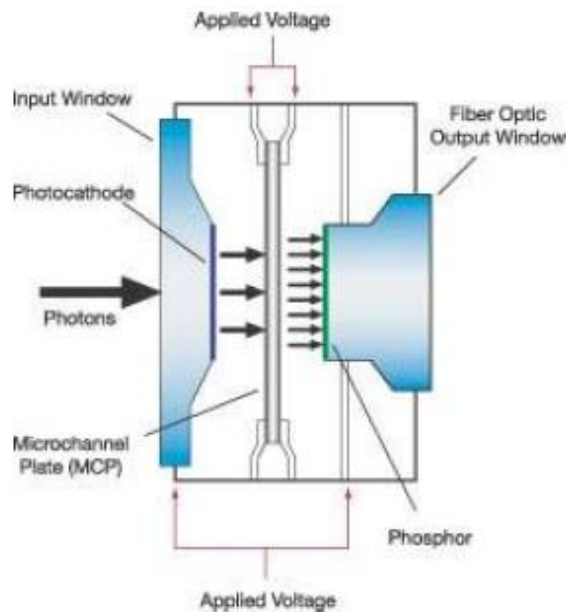


Figure 21: Intensified CCD camera from [33]

The photocathode takes the incoming photons which generate photoelectrons in the photocathode that can travel towards the MCP due to an applied electric voltage. These cameras are therefore gated, which means they can be turned on and off by modifying the electric voltage applied to the photocathode at very fast rates. By switching the voltage, the photoelectrons located in the photocathode can achieve the required velocity to move down to the MCP (ON state), or they cannot move to the MCP, therefore the phosphor screen will not receive any electron (OFF state). If the electrons leave the photocathode, depending on the applied voltage on the MCP, arriving electrons can dislodge secondary electrons from the MCP, which increases the number of electrons reaching the phosphor. By changing the gain (or voltage applied) to the MCP the number of electrons that get to the phosphor can be modified [33]. Therefore, if the signals that are trying to be acquired are too low, by increasing the gain in the MCP, a greater signal will be retrieved.

The camera used in this experiment was designed to achieve nanosecond gating times. Specifically, the one used, was able to switch on and off the intensifier as fast as $< 2ns$ gate times. This makes this camera very precise in time which makes it possible to take images in the nanosecond range, a very important characteristic for this work, since nanosecond lifetimes are typical of fluorescence.

2.1.6.1. Signals from the Camera

To understand how the camera works, a look into the electrical signals the camera uses might be helpful, so an oscilloscope was used to look at the signals in a visual and easy way. Each of the signals has an SMA connector in the back of the camera, which were connected to the oscilloscope. In order to see the Gate Monitor in the oscilloscope a different connector is required different to the SMA one used for the other signals. It is provided by the supplier and it has a BCN connector at the other end to attach it to the oscilloscope. The signals can be seen in *Figure 22*.

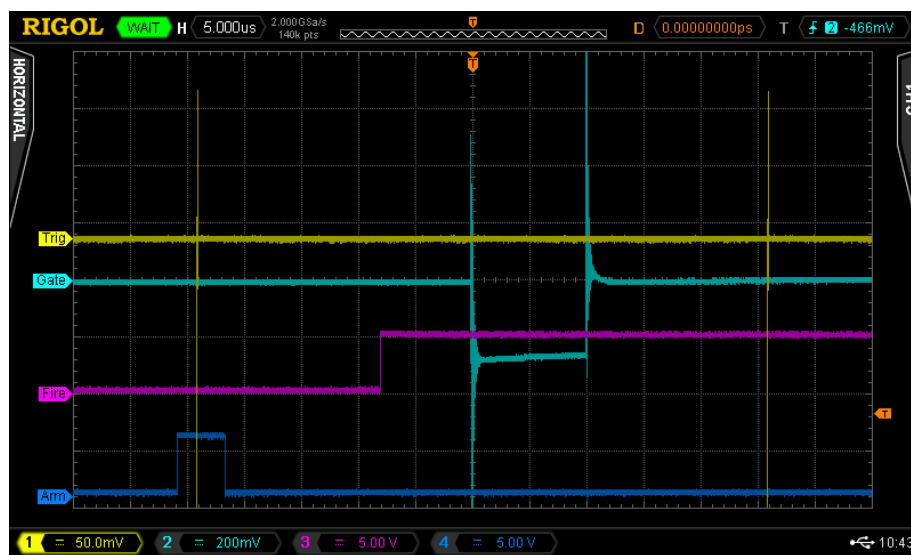


Figure 22: Signals from the camera from [34]

- *External Trigger (yellow)*: used to initiate data acquisition with an external device and it can only be accepted by the camera if Arm signal is high.
- *Arm (navy)*: high when the camera is ready to accept external triggers.
- *Fire (purple)*: determines the time the camera is acquiring an image. It is high (5V) when the light is allowed to pass to the CCD, so it can be integrated, on the other hand is low (0V) when no light is getting to the CCD.
- *Gate (blue)*: allows for monitoring of the photocathode switch on and off state. Electrons are getting to the MCP between the low (ON) and high (OFF) peak. (It can be understood as the time lapse when the image is taken.)

The camera has different ways of controlling the intensifier gating. During this work, the gate mode used was Digital Delay Generator (DDG). The DDG activates when an

internal (fire pulse) or external trigger takes place. In this mode, the intensifier is on only when the gate pulse is high. DDG are electrical signals that allow for synchronization with different devices and they can also be measured using an oscilloscope with the SMA connectors located in the back of the camera. Depending on the application different DDG signals will be used. Using the Gate Delay, the gate pulse can be chosen to occur at a specific time, opening the image intensifier only at the desire time during the exposition. Gate Width refers to the time the image intensifier remains open, and both these parameters can be modified from 0 to 10s in 10ps steps. The last DDG used in this work was Output A, which is an auxiliary output pulse specifically designed to synchronize triggers for other devices. It also allows for delays between 0 to 10s and widths between 2ns to 10s in 10ps steps[35].

Output A was used as a trigger for the laser to start oscillating since according to the supplier it was the most reliable signal that could be obtained from the camera. It was set to match the exposition signal (fire), with no delay between them, and equal width.



Figure 23: CH1 (yellow): Output A, CH2 (blue): Gate monitor

2.1.7. DAQ

In order to coordinate all the different parts, a Data Acquisition (DAQ) device was used. The one chosen was obtained from National Instrument USB-6341, with 16 Analog Input (AI) channels, maximum sampling rate in the AI of 500kS/s, 2 Analog Output (AO) channels, with maximum resolution of 900 kS/s, 24 Digital Input/Output (DIO) channels and a maximum clock rate in the DIO of 1MHz.

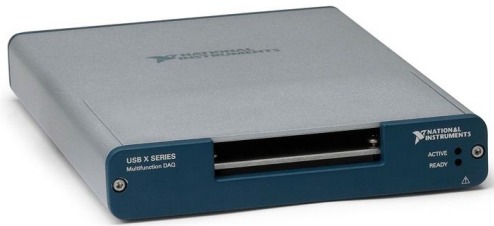


Figure 24: USB-6341, National Instruments from [36]

It was used mainly as a coordination element for the whole process. It was in charge of receiving the Output A signal from the camera in one of the DI channels. This signal was used as a trigger for starting the sinusoidal wave, which had to be given as the RF frequency to the AOTF (using one of the AO channels), allowing amplitude modulation of the laser.

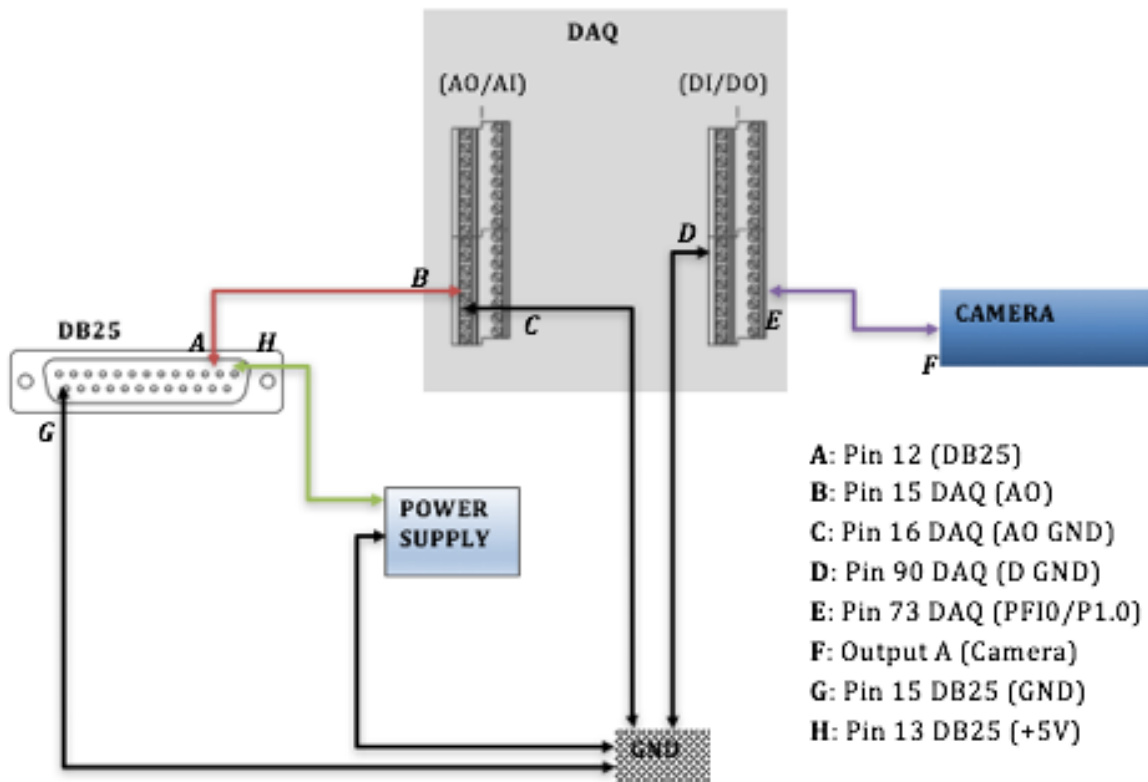


Figure 25: Schematic for the wiring process.

2.1.8. Software Design

Software provided by the manufacturers of some of the components was used such as MDS software and Andor Solis. Apart from this, a program using LabView was developed to let the user control the different modulation frequencies.

Although the AOTF was used in external mode, the MDS software was required to store the parameters needed for external use. MDS software was developed by AA Opto-electronic to provide control over their range of RF-drivers.

A LabView (Laboratory Virtual Instrument Engineering Workbench) from National Instruments was created to coordinate the acquisition process. LabView is an engineering software that provides fast control of hardware and software, helping in the process of solving engineering problems in a faster way. LabView uses a visual programming language which makes it easier for inexperienced users to develop higher complex programs than with traditional programming languages [37]. A LabView program was created to control the laser modulation over a wide range of frequencies.

To control the ICCD camera Andor Solis, a software provided by ANDOR was used. Andor Solis is a software designed for image capture and analysis, for many different fields such as Raman imaging, fluorescence imaging, X-rays studies... Andor Solis provides total control of the camera's parameter such as horizontal and vertical binning, read out time and exposure time to name a few. The control can be done manually by using the software, however, they also give the possibility to write programs that can run automatically with their programming language Andor Basic. The different parameters needed for acquisition as Output A delay and width, Gate Delay and Gate Width, as well as the gain on the MCP can be set using Andor Basic [38].

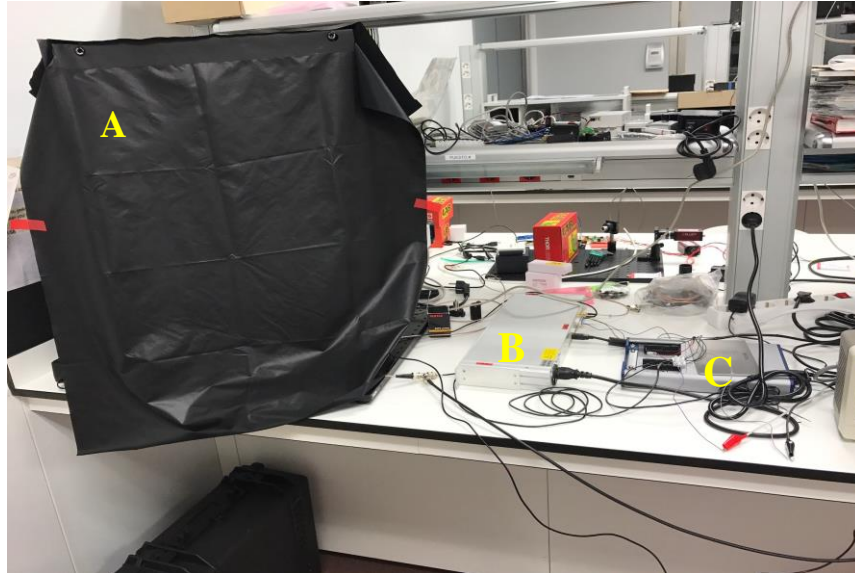
Matlab is a programming language used by scientist and engineers that allows for matrix manipulation, functions and data representation as well as algorithm implementation [39]. In this project Matlab simulations were performed to graphically see the relation between demodulation and phase shift with respect to the modulation frequency for different lifetimes.

2.2. Final System Assembly

Different components have been coordinated for the development of this work, and the explanation of how each of them work has been given in the previous section, however, in order to understand the project as a whole, the final system assembly will be shown, as well as a schematic of the final system for clarifying purposes.

In Figure 26 (A) it can be seen that the detection system has been covered by a light proof structure. with thick black cardboard on two of its side, and with black fabric in the front and top. The use of black fabric in this two side was to give easy access to the sample and to the camera connectors. Covering the detection was require due to the high sensitivity of the camera. Even light coming from the lab could cause irreversible damage in the MCP, therefore avoiding unwanted illumination was required.

(A)



(B)

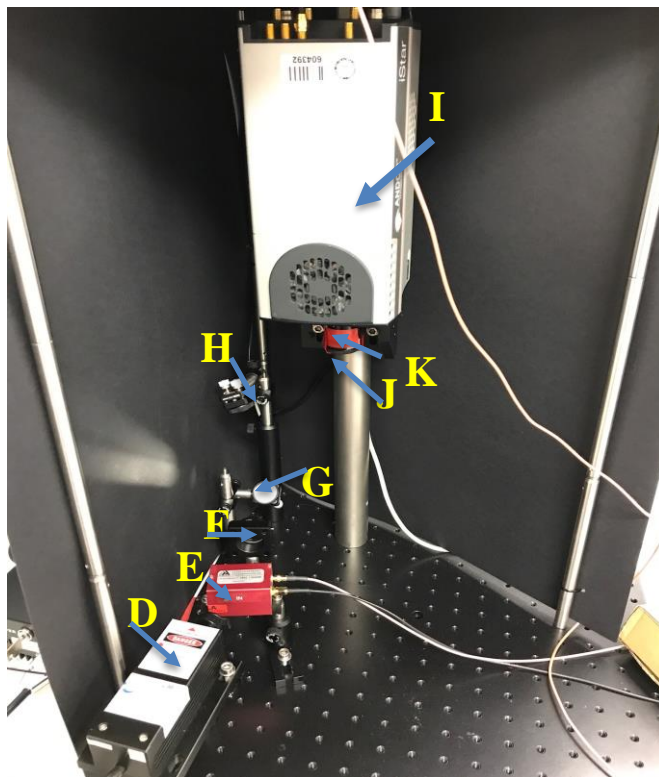


Figure 26: (A) Final System Assembly: A-Detection system, B-MDS, C-DAQ. (B) Close up to the detection system: D-Laser, E-AOTF, F-Lens, G&H- Mirrors to redirect the path of the diffracted light, I- ICCD camera, J- Emission filter, K- Objective.

A simplified schema of the final system is given below for clarification purposes.

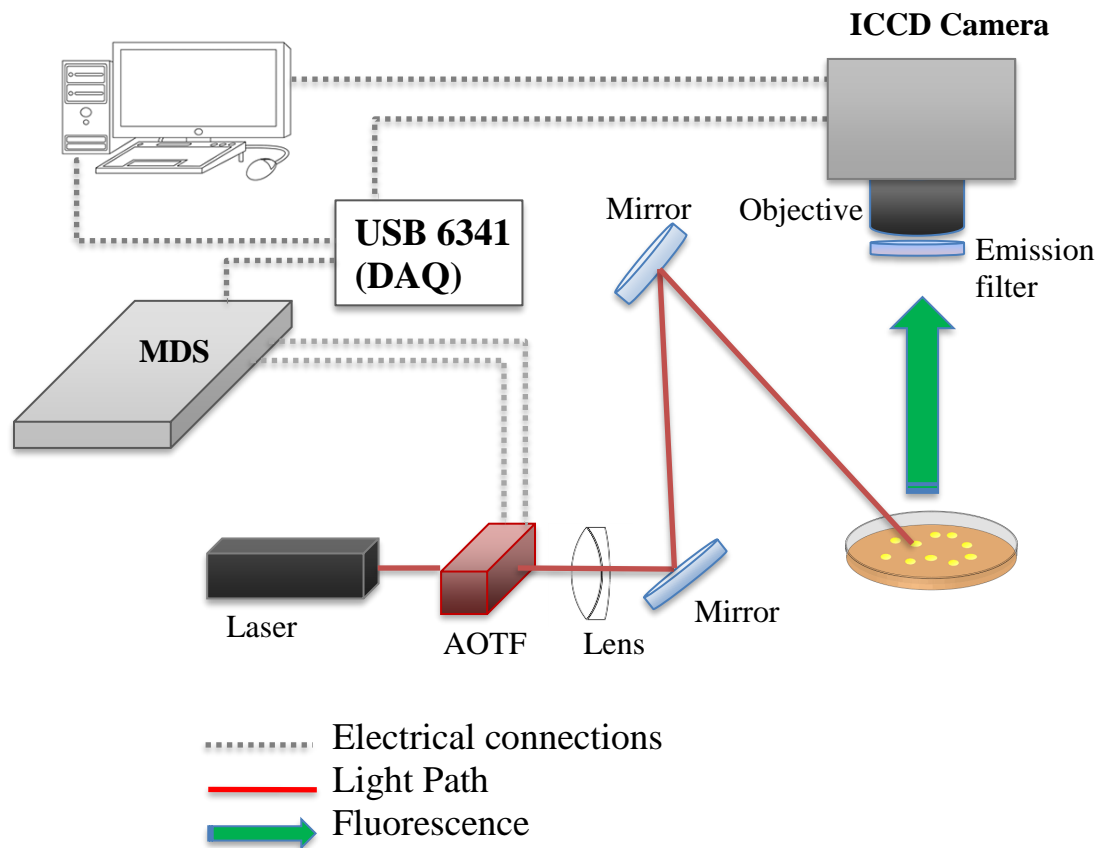


Figure 27: Schematic drawing of final system assembly

2.3. System Initialization Protocol

To ensure the correct functioning of the system, several steps have to be followed.

1. Connect the RF OUT and Therm Stab cables from the MDS to the AOTF.
2. Turn ON the power button in the MDS and wait for 15 for system stabilization.
3. Connect the USB of the MDS to a computer.
4. Initialize the MDS software.
5. Select the CONNECT button and choose the COM port (\\Device\\USBSERxxx)
6. Select CHANNELS ON/OFF
7. Change to INTERNAL MODE and look for the channel that gives better separation angle between 0th and 1st order diffraction.
8. Once the channel for best separation is found, change the frequency to be the one in CHANNEL 1
9. Turn ON CHANNEL 1.
10. Turn OFF the rest of the channels.
11. In the EXTERNAL COMMAND VOLTAGE select 5V.
12. Select STORE to save the parameters (CHANNEL 1: ON, EXTERNAL COMMAND VOLTAGE: 5V)
13. Connect external power supply (5V) and DAQ.
14. Turn on laser.
15. Change to EXTERNAL MODE.
16. Connect the camera to the power supply and turn it on.
17. Connect USB from the camera to a computer (USB 2.0 required).
18. Open Andor Solis software.

- 19.** Start LabView program.
- 20.** Select modulation frequency on LabView program
- 21.** Run acquisition in Andor Solis.

3. Results and Discussion

3.1. Laser modulation

In order to modulate the laser, the AOTF was used. As previously mentioned, the MDS had the option to be controlled through internal or external mode, and external mode is required if the objective is to modulate the intensity of the laser. Once the adequate channel was chosen in internal mode, the MDS driver was changed to external control, and a sinusoidal wave generated using the DAQ was used as the modulation input.

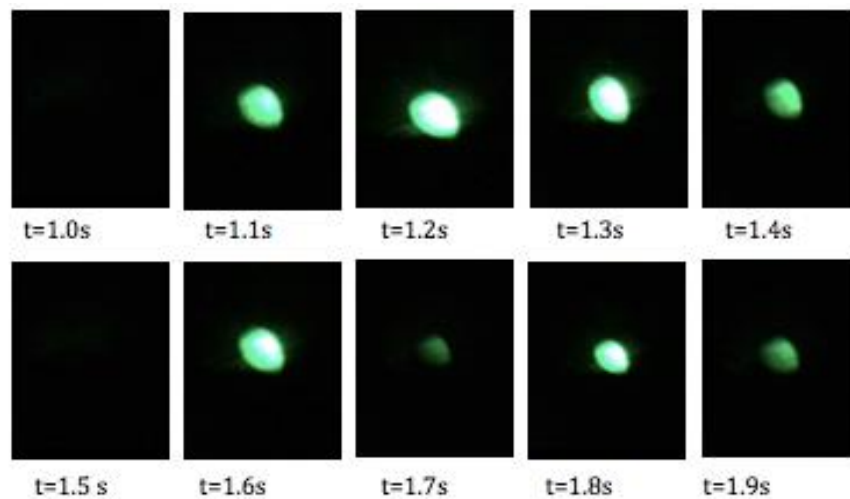


Figure 28: Images obtained from a video showing the laser modulation. Frequency of modulation: 10Hz.

To check further that the frequency generated by the DAQ was accurate, an oscilloscope was used to measure the wave coming from the DAQ, as well as the RF out from the MDS, to prove that the frequency getting to the AOTF was equal to the one generated (Figure 29). Different frequencies were tried, until higher frequencies could not be generated by the DAQ, finding the maximum frequency to be 300kHz without aliasing.

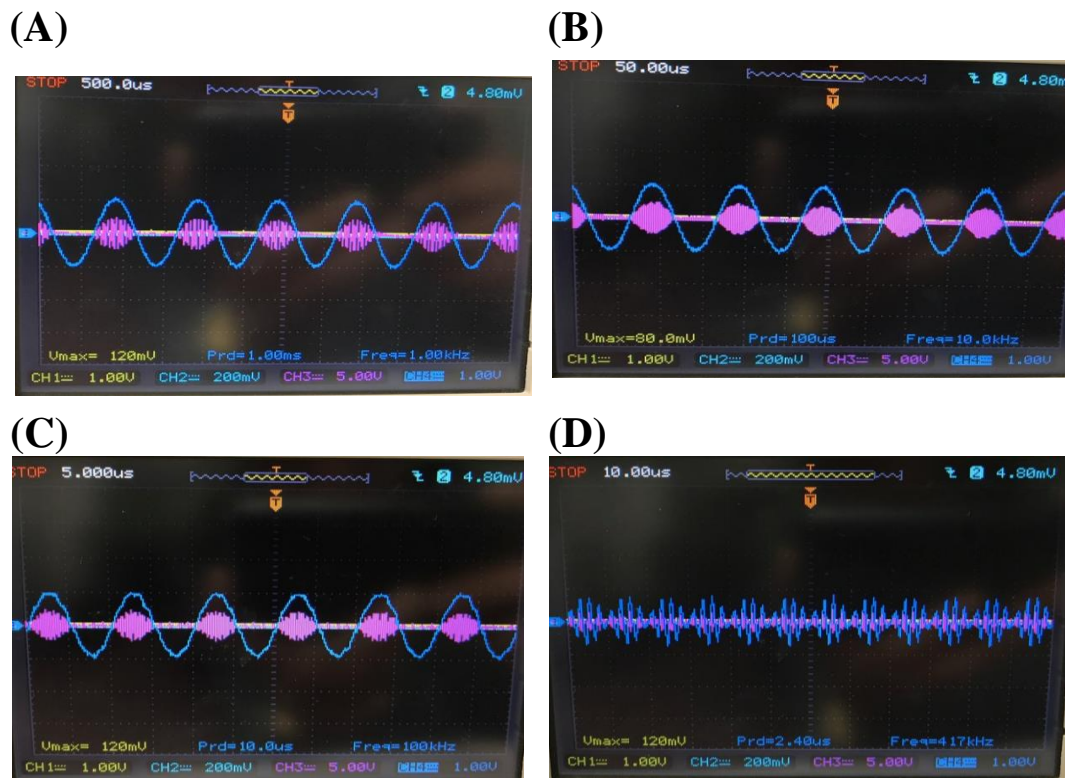


Figure 29: (A) $f=1\text{kHz}$, (B) $f=10\text{kHz}$, (C) $f=100\text{kHz}$, (D) $f=400\text{kHz}$. CH4 (blue): signal measured from analog output from the DAQ. CH3 (purple): signal measured from RF OUT from MDS.

Figure 29 shows sine waves generated at different frequencies, but in order to further prove that the modulation of the laser was done correctly, a photodetector was used to measure the real modulation of the laser right after the AOTF at different frequencies. The photodetector system was developed by Miguel Ángel Lorente Fernández and it has a power supply, as well as the connector needed for monitoring the output signal using an oscilloscope. The set up used with the photodetector can be seen in Figure 30, and in the next figure, different images show that the laser modulation follows precisely the sine wave generated by the DAQ.

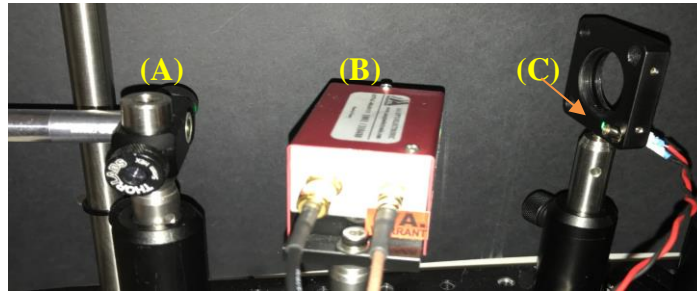


Figure 30: (A) Laser, (B) AOTF, (C) Photodetector

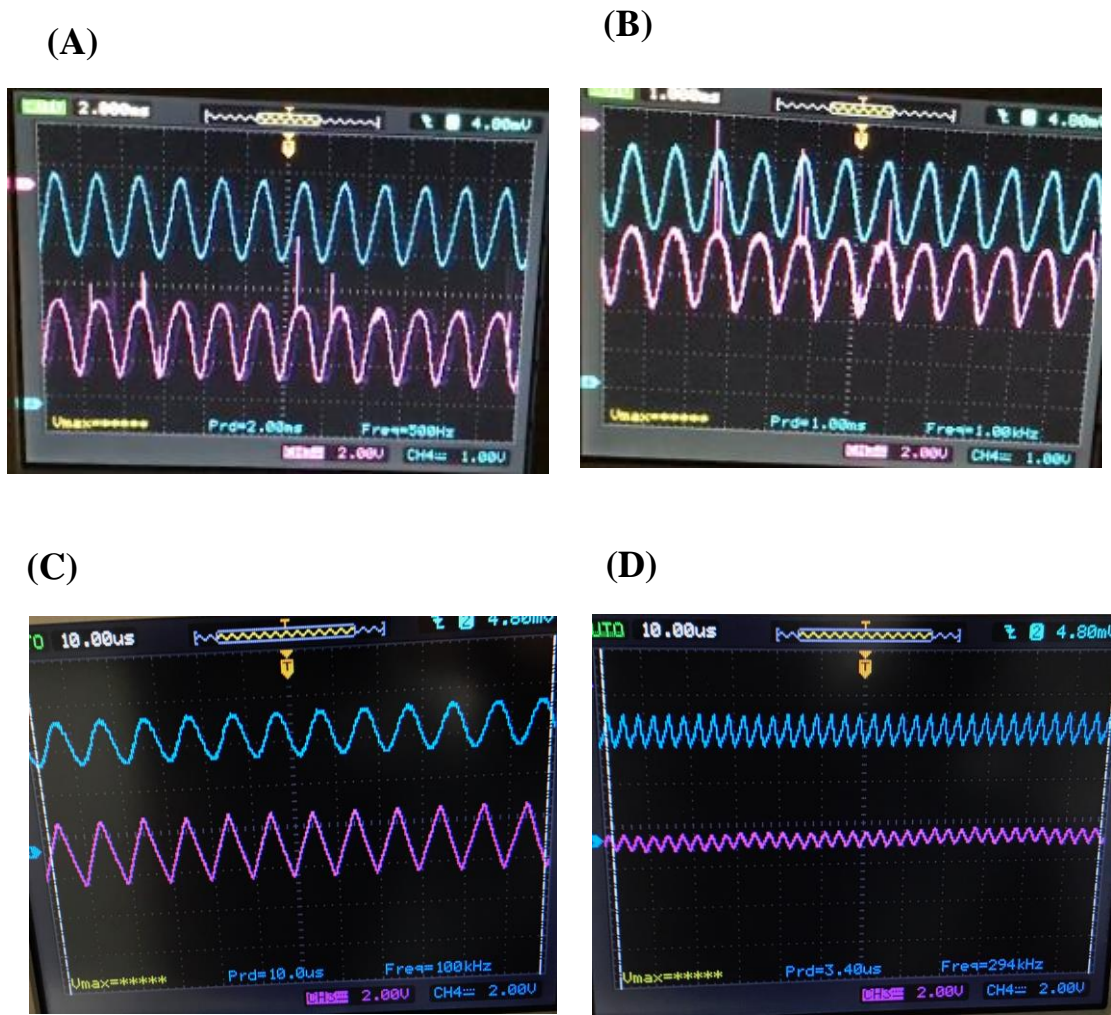


Figure 31: In all images, the **blue signal** (CH4) corresponds to the signal generated by the DAQ, and the **purple signal** (CH3) corresponds to the signal obtained from the photodetector. Different frequencies were measured (A) $f=500\text{Hz}$, (B) $f=1\text{kHz}$, (C) $f=100\text{kHz}$, (D) $f=300\text{kHz}$

3.2. Camera and laser coordination

Two different ideas were considered to coordinate the acquisition system. Since precision in the time were the images were taken was required, it was important to check if it was possible to obtain images accurately throughout the emission wave.

The first approach was to turn the laser on and off between images acquisition. In order to do this, the time it took the laser to start oscillating had to be constant. If this was the case, it would be possible to ensure that images were always taken at the desire delay every single time. However, by checking the delay between the exposition time of the camera (using Output A) and laser initiation, it was clear that the time was not constant (*Figure 32*), probably due to a non-optimal implementation of the LabView program, which introduced variable delays between the trigger signal (Output A) and the laser oscillation start. Since the start time of the laser was not reliable, it would not have been possible to accurately know where the different images were taken, making reconstruction of the fluorescence lifetime signal impossible.

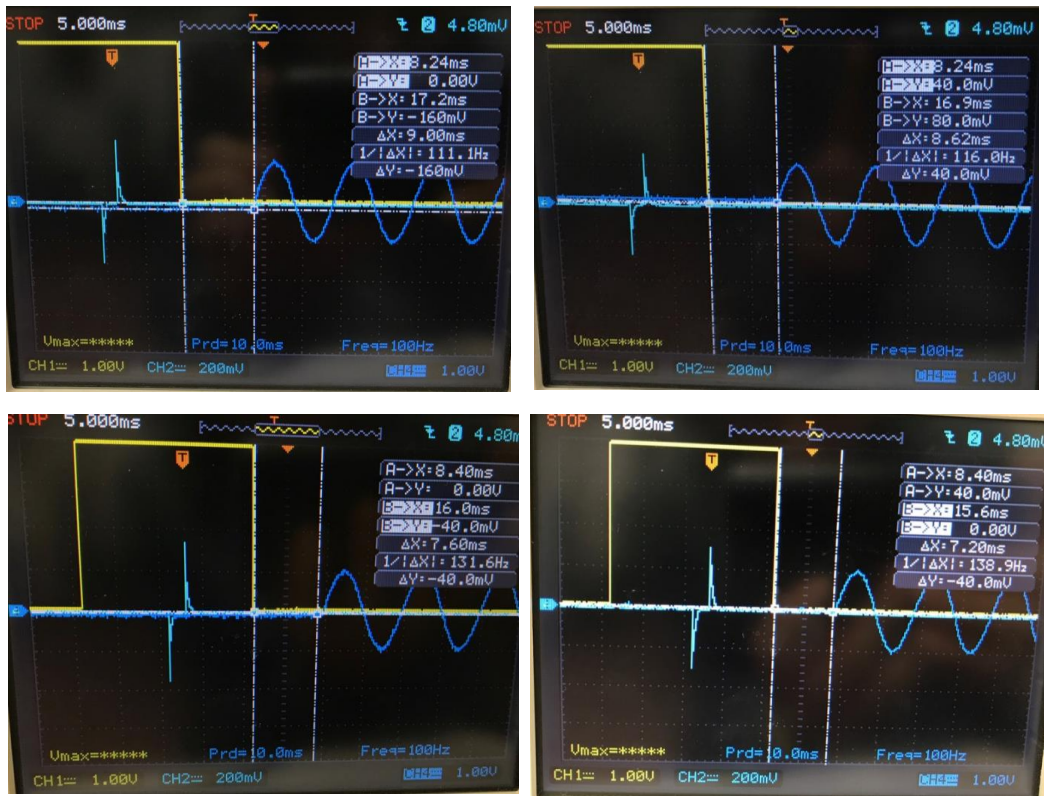


Figure 32: Same exposition time (20ms) and gate delay (10ms) were used in all images. The delay between Output A (CH1) and the sinusoidal wave (CH4) varies in each image (ΔX).

Therefore, a second approach was presented, were the laser will start oscillating when the first trigger coming from the first images (Output A) gets to the DI pin in the DAQ, and it keeps oscillating for the whole acquisition time, in this way the variability of oscillating start is solved, since images are taken after that variable time. Following this approach consecutive images will be taken at different points in the emission wave. However, because the camera is not fast enough to acquire several images in one period, images were taken consecutively but in different periods. To ensure that this was done correctly, signals of the excitation wave and the gate monitor, were looked at using the oscilloscope (*Figure 33*).

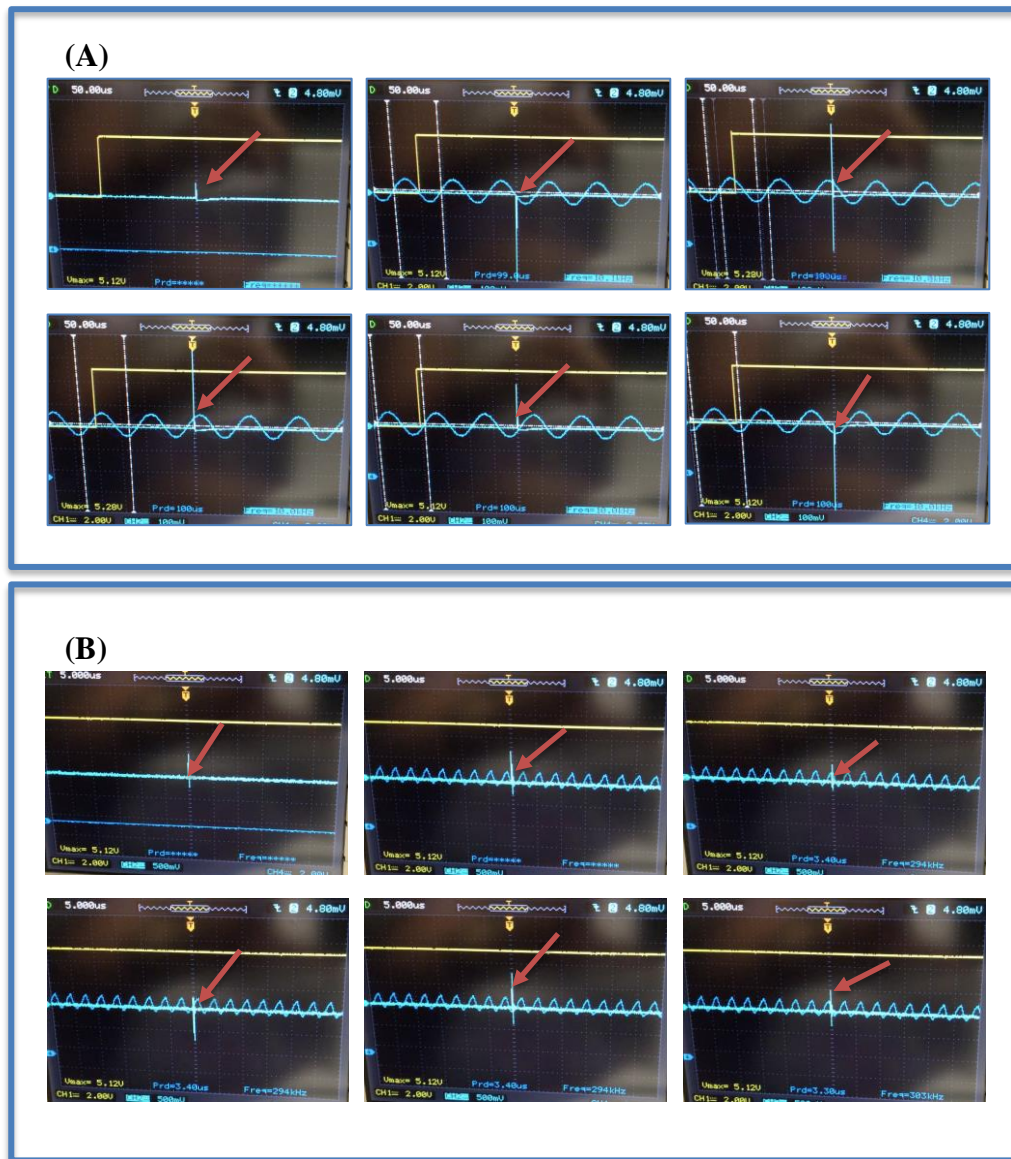


Figure 33: Sequence of images obtained from a video of the acquisition process at (A) 10kHz and (B) 300kHz. The red arrow points to the gate monitor

Looking at the red arrow, which points to the gate monitor (i.e. time were the image is taken), it can be clearly seen that images are being taken consecutively over the excitation wave.

In terms of how the camera acquired the images, *Kinetic Series* mode was used. In this mode, the camera performs several images with a fixed time (*kinetic cycle time*) between the images. The parameters selected for the acquisition were: exposure time of 0,001s, number of accumulations was set to 1, since only one image was desired to be taken each time. The gater delay was 0,2ms, and the width was set to 0,1 μ s. Output A (trigger for the laser oscillation) was selected to be the same as the exposure time, delay of 0s and width of 0,001s, since is the most reliable signal coming from the camera. These parameters were experimentally optimized to ensure that sequential images (in small steps) were taken over the emission wave.

3.3. Testing the system

To test if the system was able to give some contrast based on the lifetime, images were taken at different frequencies with a fluorophore (CF680-Maleimide). Fifteen images were taken for each frequency (1000Hz, 10kHz, 100kHz, 200kHz and 300kHz), with the previously mention acquisition method.

To check if any contrast can be appreciated a normalization of the different images was performed with the following formula:

$$I = \frac{I_{max} - I_{min}}{I_{max} + I_{min}}$$

The images obtained (*Figure 34*) showed that no contrast can be seen at the frequencies we are working with (1-300 kHz), since they are far below the desire frequencies (1-100 MHz).

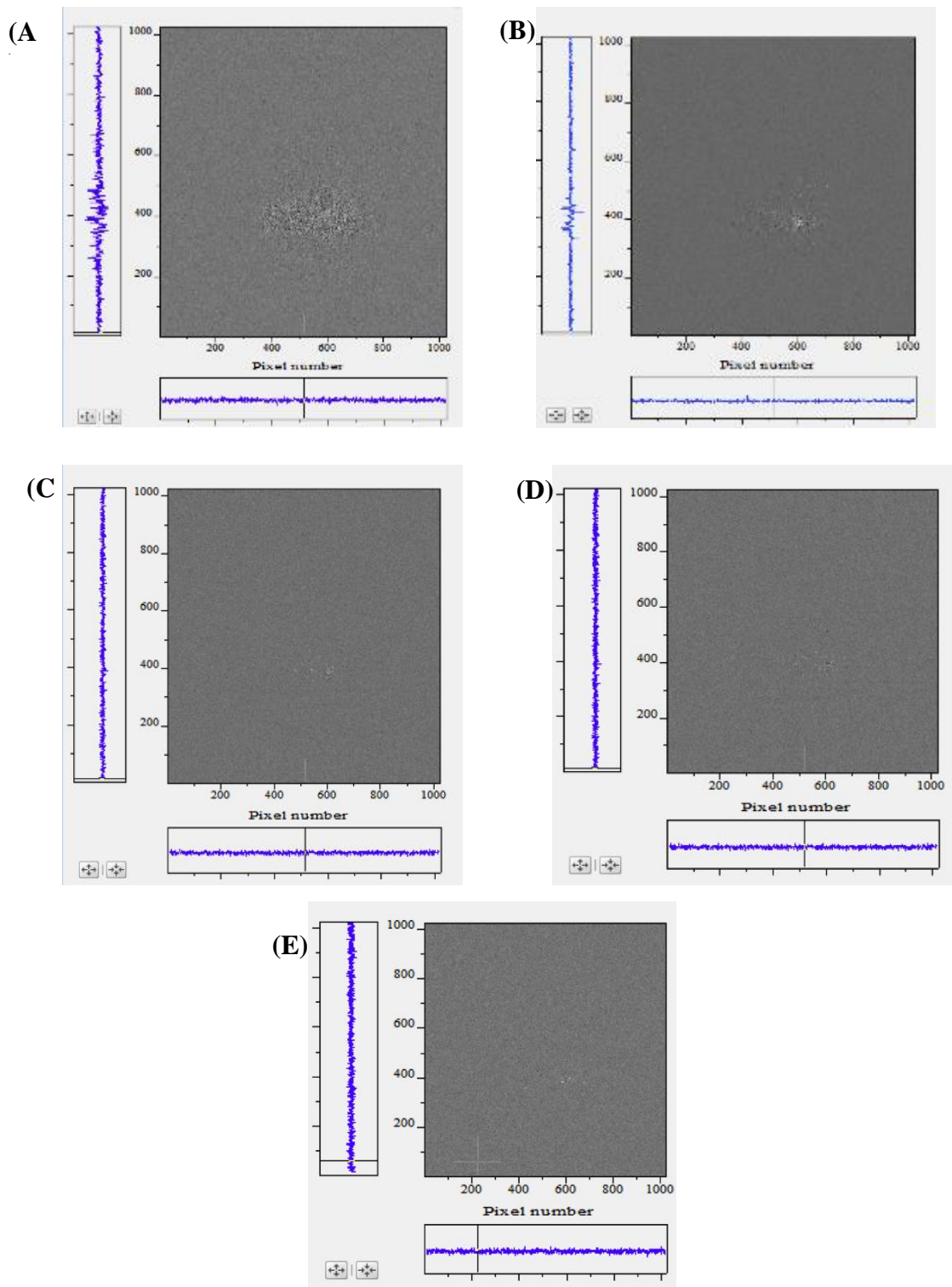


Figure 34: Normalized images of different modulation frequencies (A) $f=1000\text{Hz}$, (B) $f=10\text{kHz}$, (C) $f=100\text{kHz}$, (D) $f=200\text{kHz}$, (E) $f=300\text{kHz}$.

If the modulation frequencies were in the correct range, the demodulation and phase shift of the emitted fluorescence will depend on the modulation frequency.

At the beginning of this project simulations using Matlab were performed to understand how the demodulation and phase change will be affected by the modulation frequency for different lifetimes in the nanoseconds range. (*Annex 7.3 Matlab Code*)

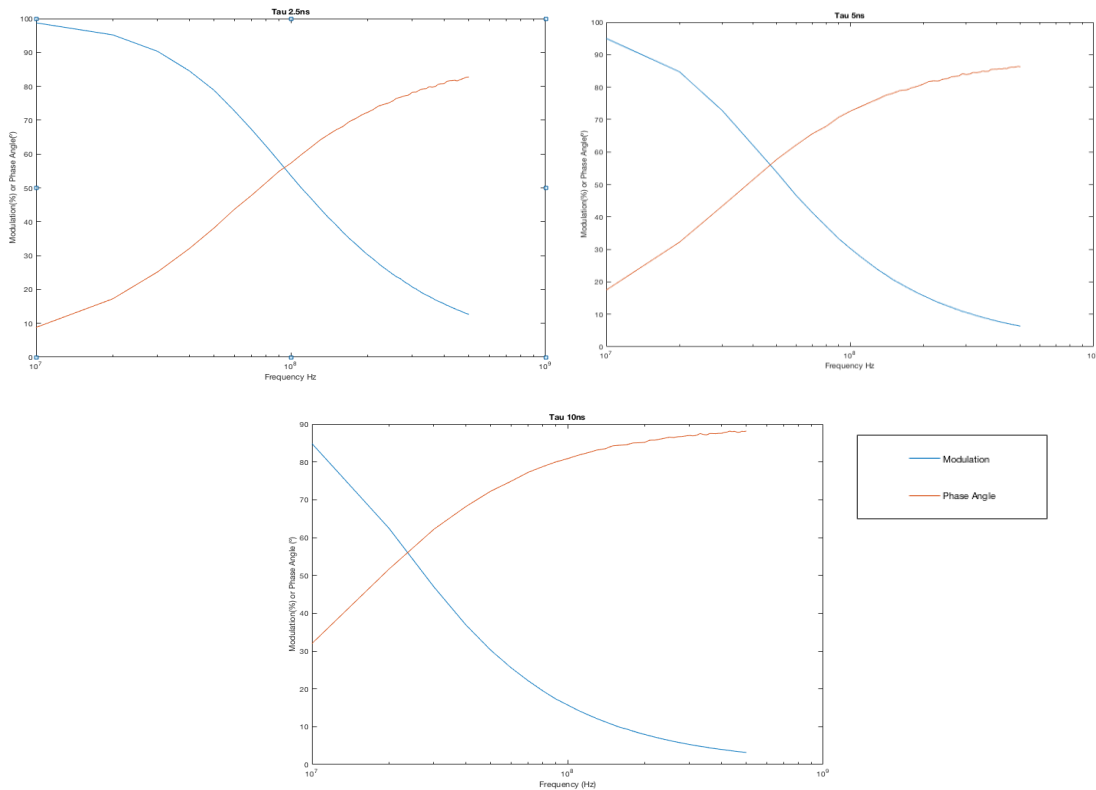


Figure 35: Simulations performed showing modulation and phase angle shift at different modulation frequencies

Looking only at the demodulation, it can be seen that demodulation goes from 1 to 0, decreasing when the modulation frequency increases. If two different modulation frequencies were chosen, were the demodulation was different enough, contrast could be appreciated in an image.

The system is therefore limited by the hardware. The inability of generating frequencies higher than 300kHz with the DAQ device at our disposal, makes it

extremely hard to look for contrast based on lifetimes in the nanosecond range. A modulation system that allows for higher frequency generation will be required, if fluorescence lifetime in the nanosecond range is desired to be used as the contrast for this system.

4. Conclusion

4.1. Current State of the System

The system has been fully assembled and all the connections needed for the different components to be coordinated have been implemented. A LabView program has been created for user friendly control of the modulation frequency. A light proof cage has been built to protect the camera from undesired light to be captured during acquisition, as well as easy access to the sample and the different optical components for manipulations have been ensured. The lens and mirrors have been mounted to allow for homogeneous illumination of the sample.

In terms of the capabilities of the system, it has been proved that intensity-modulation of the laser was possible using an AOTF at kHz frequencies, and sequential image acquisition at different modulation frequencies have been demonstrated. However, limitations have been encountered with the hardware, in particular with the DAQ, which doesn't allow for Megahertz frequencies generation, which has make it extremely hard to see contrast based on lifetime.

4.2. Next Steps

Future work should be primary done in getting MHz modulation frequencies for the light source. Once the modulation is implemented and acquisition is checked to still work at those higher frequencies different experiments should be tried to further test the capabilities of the system. Experiments changing the pH of a solution containing a fluorophore would be an easy way to test if the system is able to detect contrast. If higher precision was required, it could be possible to develop a program for reconstruction of the emitted fluorescence. As explained in the introduction of this project, the fluorescent molecule will emit with the same modulation as the excitation, therefore if several images were taken over a period, reconstruction of the sinusoidal emitted wave should be possible. By measuring the phase shift and the demodulation with respect to the excitation, determination of the lifetime of a fluorophore should be possible.

Since the final purpose of the system was to use it in in vivo applications, autofluorescence will be easily removed in the sample, to allow for easier detection of the targeted fluorophore using this system. Therefore, testing the system in in vivo experiments would be also a good continuation for this bachelor thesis.

5. SOCIO-ECONOMIC IMPACT

Lifetime measurement is still a relatively new technique, which opens a new way of understanding fluorescence imaging. Intensity-based fluorescence methods have been widely used for many different applications for the past decades. However, intensity measurements are dependent on fluorophore concentration, photobleaching and quenching. Measuring lifetime, which is not affected by any of these phenomena, can provide more in-depth knowledge on molecular environment. Molecule binding such as protein interactions can be study using FRET-FLIM techniques, and pH, O₂ or Ca²⁺ sensing will allow for further and faster understanding of different molecular processes, which will be very helpful in biology and chemistry applications.

Another potential application of fluorescence lifetime imaging, that will simplify the actual methods for measuring fluorescence, is the ability to measure the lifetime of targeted probes on in-vivo experiments of highly autofluorescence environments. Autofluorescence will be easily removed, improving the contrast in the images acquired. This can potentially simplify in-vivo experiments, reducing the time needed for their development.

6. PROJECT COST

The budget of this project is divided in three different sections corresponding to system components, technical equipment and human resources. System component is understood as all the material needed for the set-up of the acquisition system. For the electronic components, a five years life has been used to estimate the cost per year.

System Components	Quantity	Cost/Unit (€)	Cost/Year (€)	Dedication (hours)	Total Cost (€)
Camera- DH334T-18U-03 (<i>Andor Technology</i>)	1	30.000	6000	70	47,94
Multi Digital Synthesizer & AOTFnc- 400.650-TN (<i>AA Opto-electronic</i>)	1	2.000	400	100	4,56
Connector DB25	1	1	-	-	1
Lens- AC254-100-A-ML - f=100 mm, Ø1" Achromatic Doublet, SM1-Threaded Mount, ARC: 400-700 nm (<i>Thorlabs</i>)	1	89	-	-	89
Objective- 25,0 mm C-Mount Objektiv Pentax C2514-M (KP) / Ricoh FL-CC2514-2M - 1.4 / 25mm (<i>PENTAX</i>)	1	192,78	-	-	192,78
DAQ- USB-6341 (<i>National Instruments</i>)	1	1.483	296,6	100	3,38
Laser 671nm: MRL-III-671/1~200mW - up to 200 mW, 671 nm red DPSS laser with TEM00 mode, high power stability (<i>Changchun New Industries Optoelectronics Technologies Co.</i>)	1	600	120	70	0,96

Table 1: System components associated costs (1)

System Components	Quantity	Cost/Unit (€)	Cost/Year (€)	Dedication (hours)	Total Cost (€)
Laser 532nm: CPS532 - Collimated Laser Diode Module, 532 nm, 4.5 mW, Round Beam, Ø11 mm Housing (<i>Thorlabs</i>)	1	144	28,8	50	0,16
Power supply Laser 532: LDS5 - 5 VDC Regulated Power Supply, 2.5 mm Phono Plug, 120 VAC (<i>Thorlabs</i>)	1	77,50	-	-	77,50
Emission Filter: 700nm 50mm Diameter, OD 2 Longpass filter (<i>Edmund Optics</i>)	1	165	-	-	165
Mirror- ME1-G01 – 25.4mm Dia. Round Protected Aluminum Mirror, 3.2 mm Thick (<i>Thorlabs</i>)	2	50	-	-	100
Mirror Holder- MH25 - Mirror Holder for Ø1" Optics 2.5 - 6.1 mm Thick (<i>Thorlabs</i>)	2	13,40	-	-	26,8
Mirror Mount- KMS/M - Compact Kinematic Mirror Mount, M4 Taps for Post Mounting (<i>Thorlabs</i>)	2	33,75	-	-	67,5
Fluorophore- CF680 Maleimide (<i>Sigma Aldrich</i>)	1	250	-	-	5

781,58 €

Table 2: System components associated costs (1)

The costs generated by the technical equipment include laboratory machinery, as well as the different software and the computer hardware used in this project such as Matlab, LabView, MDS and Andor Solis.

Technical Equipment	Cost/Unit	Cost/Month (€)	Months used	Total Cost (€)
University Computer	-	10	6	60
Digital Oscilloscope-DS1104B (RIGOL)	800	10	2	20
LabView (15.0f2-64-bit) Software	0	0	6	0
Andor Solis for Imaging Software	0	0	6	0
MDS Software	0	0	6	0
Matlab	0	0	1	0

Table 3: Technical Equipment associated costs

80 €

Human resources costs comprise the salaries of the team members working on the project.

Human Resources	Hours	Cost/Hour (€)	Total Cost (€)
Student	400	20	8.000
Tutor	200	55	11.000
Laboratory Technician	200	45	9.000

Table 4: Human Resources associated costs

28.000 €

The final cost of the project was:

Concept	Total Cost (€)
System Components	781,58
Technical Components	80
Human Resources	28.000
	28.861,58 €

Table 5: Total cost of the project

7. ANNEX

7.1. Lifetime formulas derivation for FD FLIM

Excitation wave: $L(t) = a + b \sin(\omega t)$

Emission wave: $N(t) = A + B \sin(\omega t - \phi)$

Recall $I(t) \propto N(t)$ and that fluorescence emission follows an exponential law such as

$$I(t) = I_0 e^{-\frac{t}{\tau}} \rightarrow \frac{dI(t)}{dt} = -\frac{1}{\tau} I(t) + L(t)$$

By substituting the previous excitation and emission waves in the formula

$$B\omega \cos(\omega t - \phi) = \frac{-1}{\tau} [A + B \sin(\omega t - \phi)] + (a + b \sin(\omega t))$$

$$B\omega [\cos(\omega t) \cos(\phi) + \sin(\omega t) \sin(\phi)]$$

$$= \frac{-1}{\tau} [A + B \sin(\omega t) \cos(\phi) - B \cos(\omega t) \sin(\phi)] + a + b \sin(\omega t)$$

$$\begin{cases} -\frac{1}{\tau} A + a = 0 \\ B\omega \sin(\omega t) \sin(\phi) = -\frac{B}{\tau} \sin(\omega t) \cos(\phi) + b \sin(\omega t) \rightarrow \\ \omega \cos(\phi) - \frac{1}{\tau} \sin(\phi) = 0 \end{cases}$$

$$\begin{cases} A = a\tau \text{ [eq1]} \\ \omega \sin(\phi) + \frac{1}{\tau} \cos(\phi) = \frac{b}{B} \text{ [eq2]} \\ \omega \cos(\phi) - \frac{1}{\tau} \sin(\phi) = 0 \text{ [eq3]} \end{cases}$$

$$\text{[eq3] Dividing by } \cos(\phi) \rightarrow \omega - \frac{1}{\tau} \tan(\phi) = 0 \rightarrow \tau \phi = \omega^{-1} \tan(\phi)$$

$$\text{[eq2]}^2 + \text{[eq3]}^2 \rightarrow \omega^2 + \frac{1}{\tau^2} = \frac{b^2}{B^2} \rightarrow \frac{B}{b} = \frac{1}{\sqrt{\omega^2 + \frac{1}{\tau^2}}}$$

$$m = \frac{B/A}{b/a} = \frac{Ba}{ba\tau} = \frac{B}{b\tau} = \frac{1}{\sqrt{1 + \omega^2 \tau^2}}$$

$$\tau_m = \frac{1}{\omega} \sqrt{\frac{1}{m^2} - 1}$$

7.2. LabView program

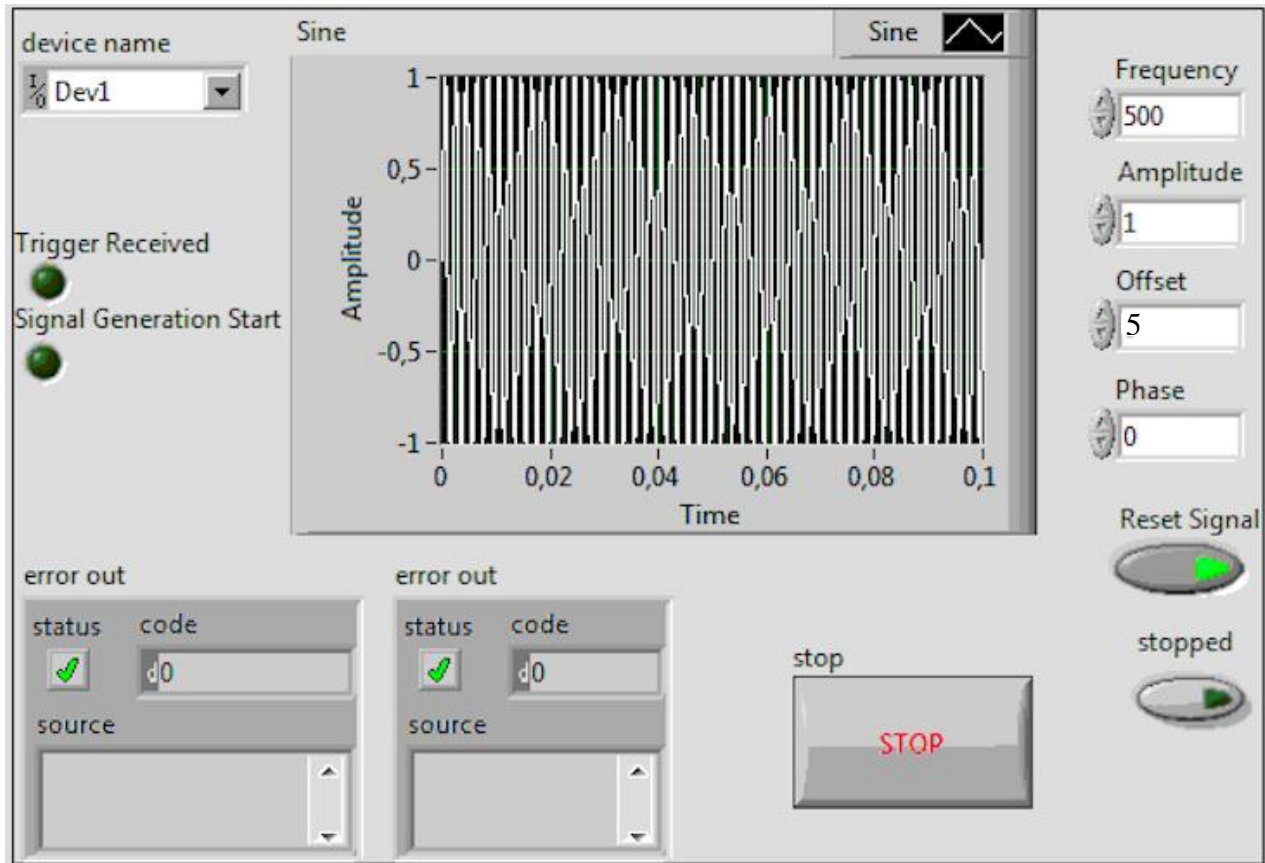


Figure 36: Control window of LabView Program

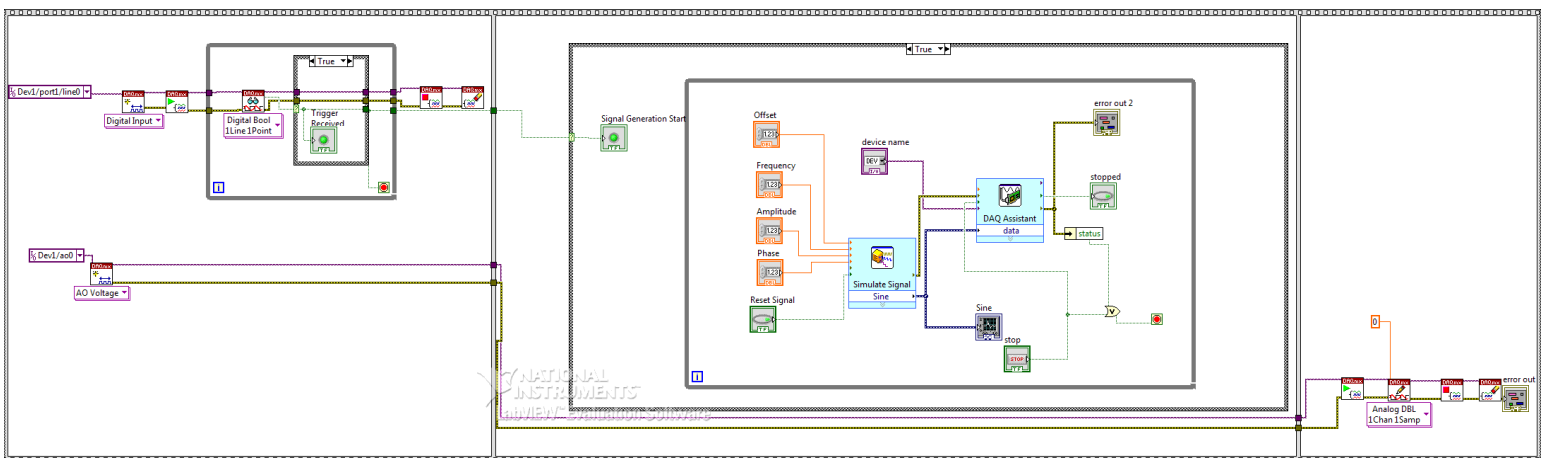


Figure 37: Terminal window of LabView program

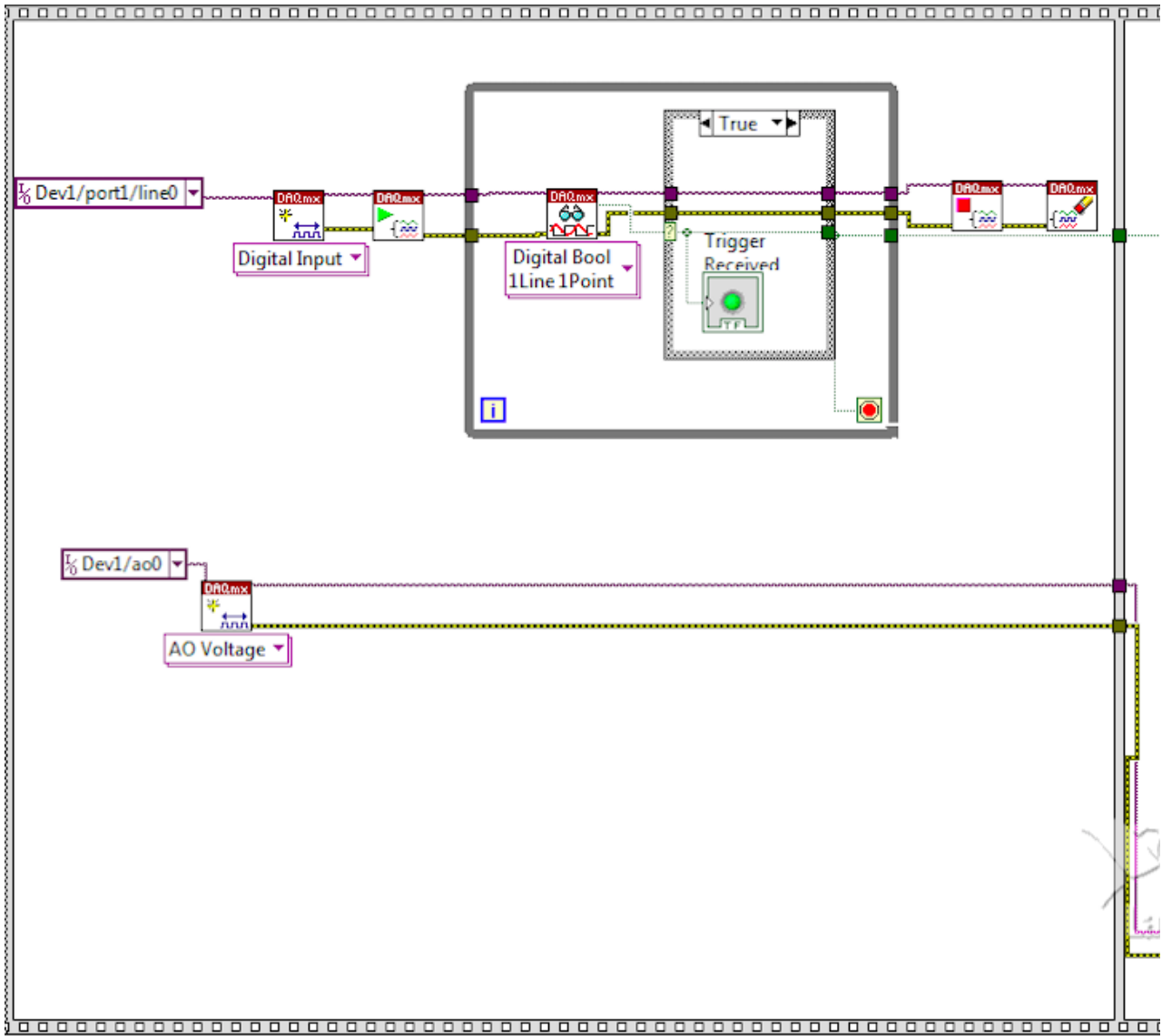


Figure 38: Terminal window LabView program (1)

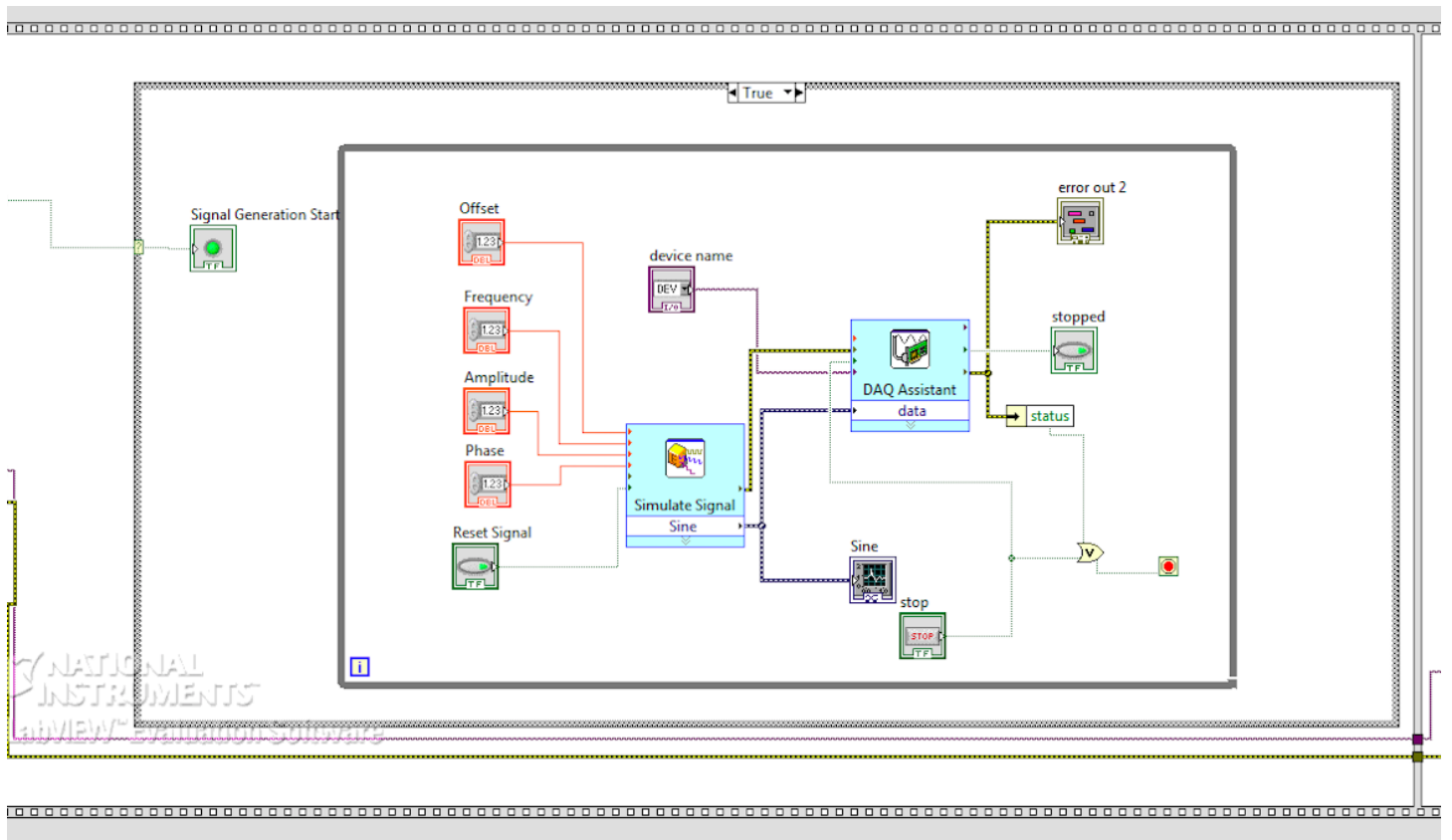


Figure 39: Terminal window LabView program (2)

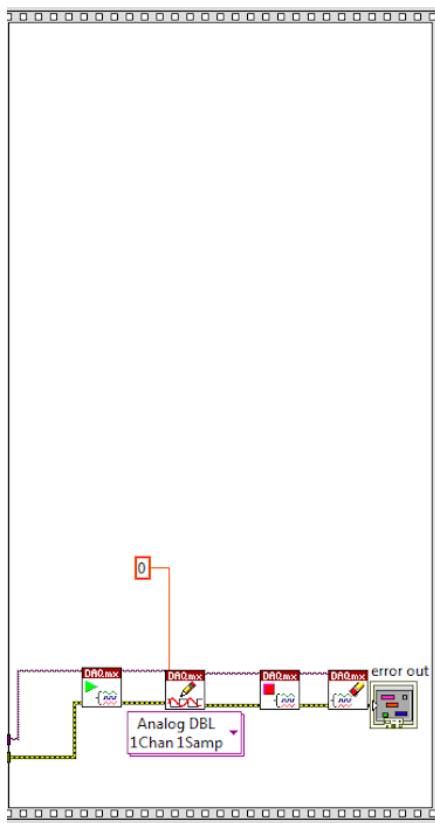


Figure 40: Terminal window of LabView program (3)

7.3. Matlab Code

Main Program

```
clear all

Fs = 10e9;      % Sampling frequency
Ts = 1/Fs;     % Sampling period
L = 1000;      % Length of signal
t = (0:(L-1))*Ts; % Time vector

%INPUT SIGNAL
f= linspace(10e6,500e6,50); %Frequencies of the input Signal (MHz)
tau=2e-9; %Change Tau to get the modulation and phase shift dependance upon frequency modulation
ValFit=[];
aoffsetEx=0; %offset of the excitation signal
bEx = 1; %amplitude of the excitation signal
yFit=[];
faseFL=[];
amFL=[];
AoffsetFL=[];

for i=1:length(f)
    w= 2*pi*f(i); %We are changing now the excitation frequency
    faseFL(i)= atan(w*tau);
    AoffsetFL(i)=aoffsetEx*tau;
    amFL(i)= bEx./sqrt((1/(tau^2)) + (w^2));
    y=amFL(i)*cos(w*t+faseFL(i))+ AoffsetFL(i);

    x0=[0,pi/2,0];

    fun = @(x)fit_function(x,y,w,t);

    [xFit]=fminsearch(fun,x0);

    ValFit(i,:)=xFit;
end

TauFaseFit=tan(ValFit(:,2)-(pi/2))./w;
TauAmpFit=1./sqrt(abs(w^2-((bEx./ValFit(:,1)).^2)));
% Since we are using the sine in the fit function but we are generating
% the wave with a cosine and sin(wt+phi)=cos(wt+phi-(pi/2));

%The phase has to be between 0-90?
%The amplitud should be between 1-0

PhaseAngle= rad2deg(ValFit(:,2)-(pi/2));
Modulation= ValFit(:,1)./(tau*bEx);

figure(2)

semilogx(f,Modulation*100)
hold on
semilogx(f,PhaseAngle)

Function

function f = fit_function(x,yData,w,t)
A= x(1);
Phase=x(2);
offset = x(3);
Ufit = A*sin(w*t+Phase) + offset;


f =sqrt(sum((yData-Ufit).^2));

figure(1)
clf
plot(t(20:120),Ufit(20:120))
hold on
plot(t(20:120),yData(20:120),'r')
```


7.4. Reference Sheet


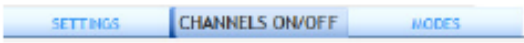
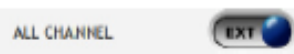
SYSTEM INITIALIZATION PROTOCOL

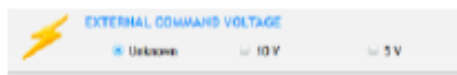
1. Connect the RF OUT and the Therm Stab cables from the MDS driver to the AOTF.



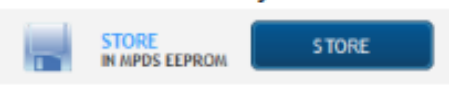
2. Turn ON the power button on the MDS device and wait for 15 minutes for system initialization.
3. Connect the USB of the MDS device to a computer.
4. Initialize the MDS program.



5. Select the  button and choose your COM port (\Device\USBSExxxx)
6. Select Channels ON/OFF 
7. Change to internal mode by selecting 
8. Choose the frequency (channel) that gives good separation between 0th and 1st order diffraction.
9. Once the channel for best separation is found, change the frequency to be the one in CHANNEL 1
10. Turn ON CHANNEL 1 and turn OFF the rest of the channels.
11. In the EXTERNAL COMMAND VOLTAGE select 5V.



12. Select STORE to save the parameters (CHANNEL 1: ON, EXTERNAL COMMAND VOLTAGE: 5V)



13. Connect external power supply (5V) and DAQ.

14. Turn on laser.

15. Change to EXTERNAL MODE by selecting

ALL CHANNEL

EXT

16. Connect the camera to the power supply, and turn it ON.

17. Connect USB from the camera to a computer (USB 2.0 require).

18. Open Andor Solis software.



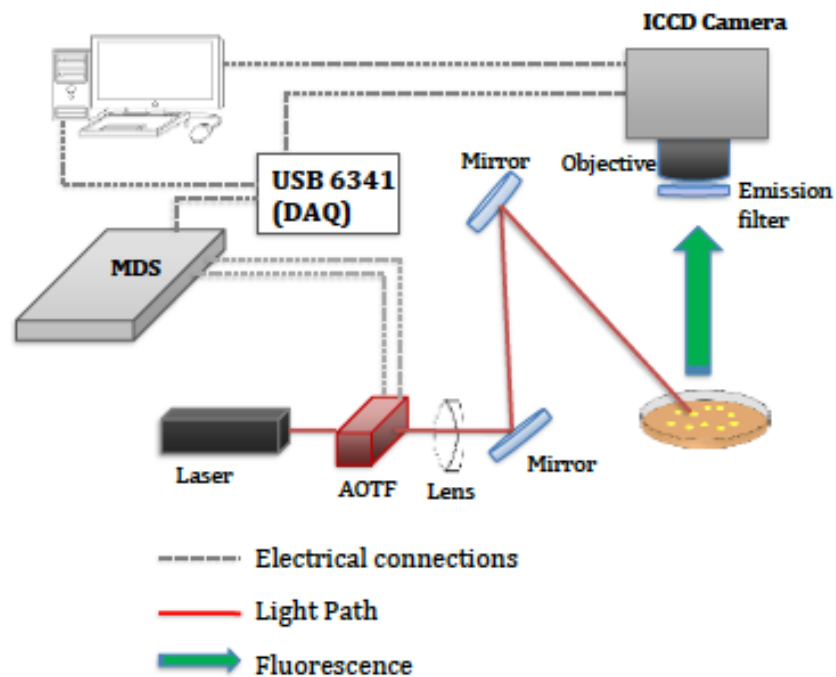
19. Start LabView program.

20. Select modulation frequency on LabView program

Frequency

500

21. Run program in Andor Solis.



7.5. Timeline of the project

The following figure shows the process that was followed for the construction of the system. It was built from scratch, nothing was previously built before the start of this bachelor thesis.

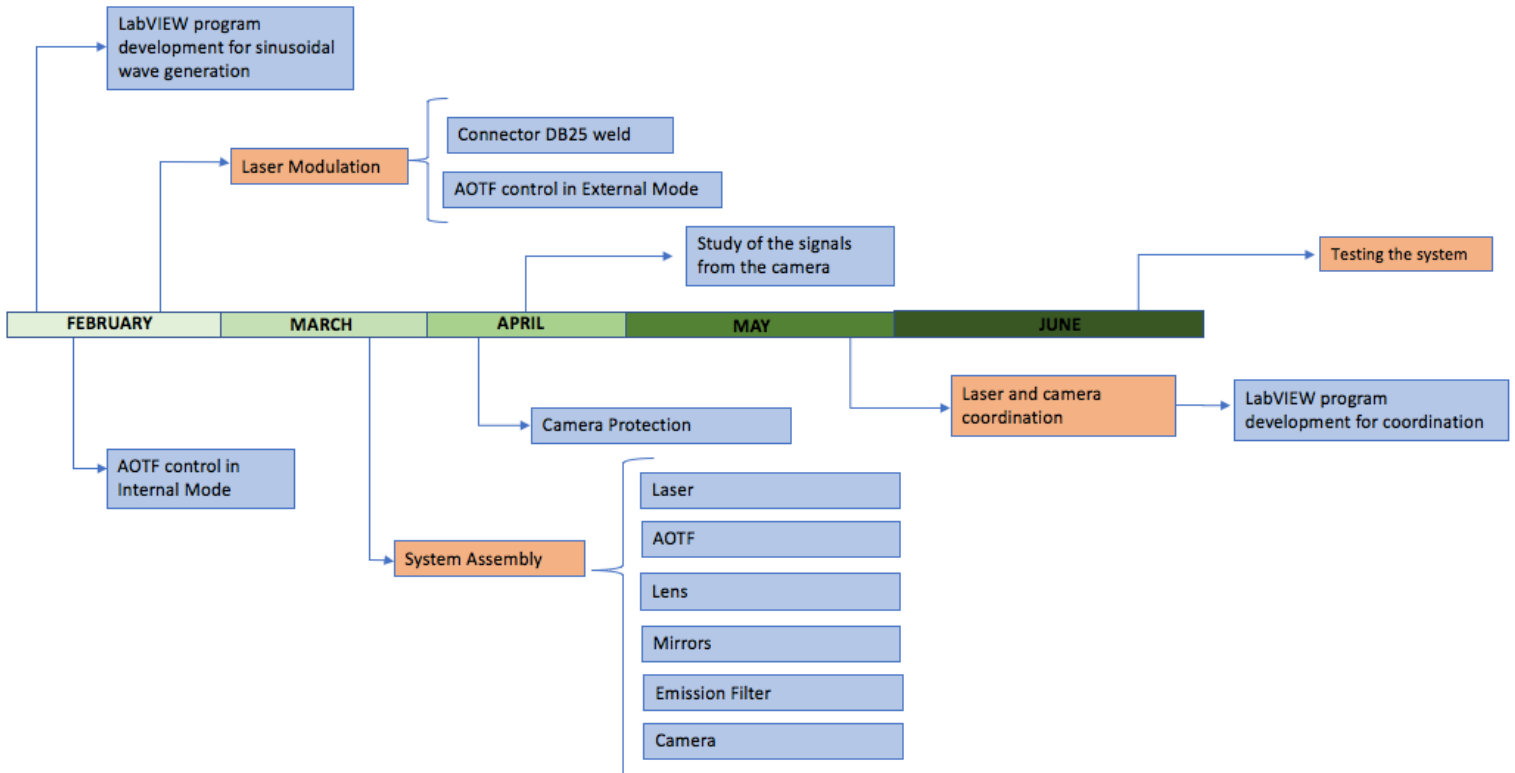


Figure 41: Timeline of the project

8. BIBLIOGRAPHY

- [1] Kobayashi, H., & Choyke, P. L. (2010). Target-cancer-cell-specific activatable fluorescence imaging probes: rational design and in vivo applications. *Accounts of chemical research*, 44(2), 83-90.
- [2] Rao, J., Dragulescu-Andrasi, A., & Yao, H. (2007). Fluorescence imaging in vivo: recent advances. *Current opinion in biotechnology*, 18(1), 17-25.
- [3] Kobayashi, H., Ogawa, M., Alford, R., Choyke, P. L., & Urano, Y. (2009). New strategies for fluorescent probe design in medical diagnostic imaging. *Chemical reviews*, 110(5), 2620-2640.
- [4] Lorenzo, J. R. (2012). Principles of diffuse light propagation: light propagation in tissues with applications in biology and medicine. World Scientific.
- [5] Abramowitz, M., & Davidson, M. W. (n.d.). Excitation and Emission Fundamentals. Retrieved from <http://www.olympusmicro.com/primer/techniques/fluorescence/excitation.html>
- [6] Teale, F. W. J. (1984). Principles of Fluorescence Spectroscopy-Lakowicz, Jr.
- [7] Briggs, S. (n.d.). Fluorescence Microscopy: In-Line Illumination with Imaging Filters. Retrieved from <https://www.edmundoptics.com/resources/application-notes/microscopy/fluorescence-microscopy-in-line-illumination-with-imaging-filters/>
- [8] Stuurman, N. (2016, August 24). Introduction to Fluorescence Microscopy: Nico Stuurman. Retrieved from <https://www.ibiology.org/ibioeducation/taking-courses/introduction-to-fluorescence-microscopy.html>
- [9] Cameras for Microscopy: Wide-Field Fluorescence Microscopy. (n.d.). Retrieved from <http://www.andor.com/cameras-for-microscopy/>
- [10] Spring, K. R., & Davidson, M. W. (n.d.). Introduction to Fluorescence Microscopy. Retrieved from <https://www.microscopyu.com/techniques/fluorescence/introduction-to-fluorescence-microscopy>
- [11] Chen, L., Lloyd, W. R., Chang, C., Sud, D., & Mycek, M. (2013). Fluorescence Lifetime Imaging Microscopy for Quantitative Biological Imaging. *Methods in Cell Biology Digital Microscopy*, 457-488. doi:10.1016/b978-0-12-407761-4.00020-8

- [12] Time-correlated single photon counting. (2015, July 21). Retrieved from http://www.photonik.uniklinikum-jena.de/en/Methods/Fluorescence_lifetime_measurements/TCSPC.html Figure reproduced from: Becker, The bh TCSPC Handbook, 6th ed., 2014.
- [13] Wikipedia collaborators (2017) Förster resonance energy transfer. Retrieved from https://en.wikipedia.org/wiki/F%C3%B6rster_resonance_energy_transfer
- [14] Berezin, M. Y., & Achilefu, S. (2010). Fluorescence Lifetime Measurements and Biological Imaging. *Chemical Reviews*, 110 (5), 2641-2684. doi:10.1021/cr900343z
- [15] Zhong, W., Urayama, P., & Mycek, M. A. (2003). Imaging fluorescence lifetime modulation of a ruthenium-based dye in living cells: the potential for oxygen sensing. *Journal of Physics D: Applied Physics*, 36(14), 1689.
- [16] Elangovan, M., Day, R. N., & Periasamy, A. (2002). Nanosecond fluorescence resonance energy transfer-fluorescence lifetime imaging microscopy to localize the protein interactions in a single living cell. *Journal of microscopy*, 205(1), 3-14.
- [17] Calleja, V., Ameer-Beg, S. M., Vojnovic, B., Woscholski, R., Downward, J., & Larijani, B. (2003). Monitoring conformational changes of proteins in cells by fluorescence lifetime imaging microscopy. *Biochemical Journal*, 372(1), 33-40.
- [18] Wagnieres, G., Mizeret, J., Studzinski, A., & Van den Bergh, H. (1997). Frequency-domain fluorescence lifetime imaging for endoscopic clinical cancer photodetection: apparatus design and preliminary results. *Journal of Fluorescence*, 7(1), 75-83.
- [19] Booth, M. J., & Wilson, T. (2004). Low-cost, frequency-domain, fluorescence lifetime confocal microscopy. *Journal of microscopy*, 214(1), 36-42.
- [20] Laser Safety Manual (UCSB Environmental Health & Safety). (n.d.). Retrieved from <http://www.ehs.ucsb.edu/files/docs/rs/lasersafetyman.pdf>
- [21] Laser Safety Manual (Iowa State University). (n.d.). Retrieved from <http://publications.ehs.iastate.edu/lserm/files/assets/basic-html/page-31.html>
- [22] Alford, R., Simpson, H. M., Duberman, J., Hill, G. C., Ogawa, M., Regino, C., ... & Choyke, P. L. (2009). Toxicity of organic fluorophores used in molecular imaging: literature review. *Molecular imaging*, 8(6), 7290-2009.
- [23] Changchun New Industries Optoelectronics Technology Co. (n.d.) MRL-III-671/1~200mW - up to 200 mW, 671 nm red DPSS laser with TEM00 mode, high power stability. Retrieved from: <http://www.cnilaser.com/MRL-III-671.htm>

- [24] Thorlabs (n.d.) CPS532 - Collimated Laser Diode Module, 532 nm, 4.5 mW, Round Beam, Ø11 mm Housing. Retrieved from:
<https://www.thorlabs.com/thorproduct.cfm?partnumber=CPS532>
- [25] Saleh, B. E., Teich, M. C., & Saleh, B. E. (1991). Fundamentals of photonics (Vol. 22). New York: Wiley.
- [26] ISOMET. (n.d.). Application Note: "Acousto-Optic Modulation". Retrieved from
http://www.isomet.com/App-Manual_pdf/AO%20Modulation.pdf
- [27] AO Tunable Filters & Fiber Pigtailed (n.d.). Retrieved from
<http://www.aoptoelectronic.com/4en.aspx?sr=4>
- [28] AA Opto-Electronic (n.d.), AOTFnC-400.650-TN. Retrieved from
<http://www.aoptoelectronic.com/4.aspx?sr=4>
- [29] Edmund Optics (n.d.) 700nm 50mm Diameter, OD 2 Longpass Filter. Retrieved from: <https://www.edmundoptics.com/optics/optical-filters/longpass-edge-filters/700nm-50mm-diameter-od-2-longpass-filter/>
- [30] SIGMA-ALDRICH. (n.d.) Product Information: CF680-Maleimide. Retrieved from: <https://www.sigmaaldrich.com/content/dam/sigmaaldrich/docs/Sigma/Bulletin/1/scj4600054bul.pdf>
- [31] Thorlabs (n.d) AC254-100-A-ML - f=100 mm, Ø1" Achromatic Doublet, SM1-Threaded Mount, ARC: 400-700 nm. Retrieved from:
<https://www.thorlabs.com/thorproduct.cfm?partnumber=AC254-100-A-ML>
- [32] PENTAX (n.d.) 25,0 mm C-Mount Objektiv Pentax C2514-M (KP) / Ricoh FL-CC2514-2M - 1.4 / 25mm. Retrieved from: <https://www.vision-dimension.com/en/lenses/ccs-mount-lenses/monofocal-lenses/pentax-c-mount-lens-fl-cc2514-2m/257>
- [33] ANDOR. (n.d.). Intensified CCD Cameras. Retrieved from
<http://www.andor.com/learning-academy/intensified-ccd-cameras-the-technology-behind-iccds>
- [34] Bonilla Escribano, P. (2015). Optical imaging in presence of scattering (Unpublished doctoral dissertation). Universidad Carlos III de Madrid.
- [35] ANDOR. (n.d.). Intensified CCDs for Nanosecond Time-resolved Imaging. Retrieved from
http://www.andor.com/pdfs/specifications/Andor_iStar_CCD_Imaging_Specifications.pdf

[36] National Instruments (n.d.) USB 6341
<http://sine.ni.com/nips/cds/view/p/lang/es/nid/209069>

[37] National Instruments (n.d.) LabVIEW Retrieved from: <http://www.ni.com/es-es.html>

[38] ANDOR (n.d.) Andor Solis. Retrieved from: <http://www.andor.com/scientific-software/solis-software-packages/solis-i>

[39] Wikipedia Collaborators (2017) MATLAB. Retrieved from: <https://es.wikipedia.org/wiki/MATLAB>